Bioorganic & Medicinal Chemistry 18 (2010) 7675–7699

Contents lists available at ScienceDirect

Bioorganic & Medicinal Chemistry

journal homepage: www.elsevier.com/locate/bmc

Discovery of {1-[4-(2-{hexahydropyrrolo[3,4-*c*]pyrrol-2(1*H*)-yl}-1*H*-benzimidazol-1-yl)piperidin-1-yl]cyclooctyl}methanol, systemically potent novel non-peptide agonist of nociceptin/orphanin FQ receptor as analgesic for the treatment of neuropathic pain: Design, synthesis, and structure–activity relationships ☆

Shigeo Hayashi *, Eriko Nakata, Asato Morita, Kunihiko Mizuno, Kenzo Yamamura, Aki Kato, Katsuyo Ohashi

Pfizer Global Research & Development Nagoya Laboratories, Pfizer Japan Inc., 5-2 Taketoyo, Aichi 470-2393, Japan

ARTICLE INFO

Article history:
Received 26 May 2010
Revised 14 July 2010
Accepted 15 July 2010
Available online 21 July 2010

Keywords:
GPCR
Nociceptin/orphanin FQ
NOP receptor-selective full agonist
{1-[4-(2-{Hexahydropyrrolo[3,4-*c*]pyrrol-2(1*H*)-yl}-1*H*-benzimidazol-1-yl)piperidin-1-yl]cyclooctyl}methanol (HPCOM)
Systemically active analgesic for the treatment of neuropathic pain
Mechanical allodynia
Peripheral/spinal cord-selective mechanisms
hERG potassium ion channel binding

ABSTRACT

Neuropathic pain is a serious chronic disorder caused by lesion or dysfunction in the nervous systems. Endogenous nociceptin/orphanin FQ (N/OFQ) peptide and N/OFQ peptide (NOP) receptor [or opioid-receptor-like-1 (ORL1) receptor] are located in the central and peripheral nervous systems, the immune systems, and peripheral organs, and have a crucial role in the pain sensory system. Indeed, peripheral or intrathecal N/OFQ has displayed antinociceptive activities in neuropathic pain models, and inhibitory effects on pain-related neurotransmitter releases and on synaptic transmissions of C- and Aδ-fibers. In this study, design, synthesis, and structure–activity relationships of peripheral/spinal cord-targeting non-peptide NOP receptor agonist were investigated for the treatment of neuropathic pain, which resulted in the discovery of highly selective and potent novel NOP receptor full agonist {1-[4-(2-{hexahydropyrrolo[3,4-*c*]pyrrol-2(1*H*)-yl}-1*H*-benzimidazol-1-yl)piperidin-1-yl]cyclooctyl}methanol **1** (HPCOM) as systemically (subcutaneously) potent new-class analgesic. Thus, **1** demonstrates dose-dependent inhibitory effect against mechanical allodynia in chronic constriction injury-induced neuropathic pain model rats, robust metabolic stability and little hERG potassium ion channel binding affinity, with its unique and potentially safe profiles and mechanisms, which were distinctive from those of N/OFQ in terms of site-differential effects.

1. Introduction

Neuropathic pain is a serious chronic disorder that is caused by lesion or dysfunction of the peripheral nervous system (PNS) or central nervous system (CNS), which evokes various and severe pains (or pain syndromes) as persisting morbid states such as allodynia elicited by innocuous levels of tactile, thermal, cold or other stimuli and hyperalgesia elicited by noxious- and mildly painful-levels of the stimuli, as well as burning pain, dull or sharp pain, and/or paroxysms.[3] The nerve injuries occur owing to various types of diseases, infections or other causes, and thereby develop the disorder that is responsible for (or defined as) cancer pain,[3d] postherpetic neuralgia,[3e,3f] diabetic neuralgia,[3g] postoperative resting pain,[3h,3i] and so on. For the treatment of neuropathic pain in clinical, general analgesics such as non-steroidal inflammatory drugs (NSAIDs) have been shown to have no or limited effects.[4a–c] The use of classical opioid analgesic drugs needs careful restriction or control owing to their adverse CNS side-effects, while many ineffective cases have been shown for the agonist or antagonist drugs.[4b–d] Therefore, new and effective pharmacological therapy against neuropathic pain has been sought and developed in the world.[3a,3c,4e–g]

Abbreviations: GPCR, G-protein-coupled receptor; N/OFQ, nociceptin/orphanin FQ; [^{35}S]GTPγS, [^{35}S]guanosine 5′-(γ-thiotriphosphate); HEK, human embryonic kidney; CHO, Chinese hamster ovary; HLM, human liver microsome; SD rat, Sprague–Dawley rat; MED, minimum effective dose; CCI, chronic constriction injury; hERG, human ether-a-go-go related gene; TNF-α, tumor necrosis factor-α; IL-1β, interleukin-1β; IL-6β, interleukin-6β; NE, norepinephrine (or noradrenaline); HPCOM, {1-[4-(2-{hexahydropyrrolo[3,4-*c*]pyrrol-2(1*H*)-yl}-1*H*-benzimidazol-1-yl)piperidin-1-yl]cyclooctyl}methanol; LAH, lithium aluminum hydride; WSCI, water soluble carbodiimide; i.e., 1-ethyl-3-(3-dimethylaminopropyl)carbodiimide hydrochloride; CDI, 1,1′-carbodiimidazole; SAR, structure–activity relationship.

☆ See Refs. 1,2.

* Corresponding author.
E-mail address: Shigeo_Hayashi@nifty.com (S. Hayashi).

0968-0896/$ - see front matter © 2010 Elsevier Ltd. All rights reserved.
doi:10.1016/j.bmc.2010.07.034

On the other hand, nociceptin[5a]/orphanin FQ[5b] (N/OFQ[†]) is an endogenous heptadecapeptide, and nociceptin/orphanin FQ peptide (NOP) receptor [opioid-receptor-like-1 (ORL1) receptor, or the fourth opioid peptide (OP4) receptor][6a,6b] is a G-protein-coupled receptor (GPCR) that has high homology to the classical opioid peptide receptors such as μ-, κ-, and δ-opioid peptide receptors (MOP, KOP, and DOP receptors, respectively). N/OFQ peptide and NOP receptor are widely distributed in various regions in living body, thus the central and peripheral nervous systems and other peripheral tissues, for example, brain, spinal cord, dorsal and ventral horn of spinal cord, peripheral sensory ganglia neurons such as dorsal root ganglia (DRG) neurons, smooth muscles, the immune systems, which are deeply associated with the sensory and pain perception as well as pain symptoms.[7] Significantly, the analgesic activities of N/OFQ peptide–NOP receptor system have been reported, that is, N/OFQ has displayed spinal and peripheral (but not systemic) antinociceptive activities in rodents or primates for acute pain or inflammation models,[8a–g] and for neuropathic pain models such as peripheral nerve injury,[9a–c] spinal cord injury,[9c] diabetes,[9d] peripheral nerve section,[9e] and postoperative pain[9f] models.

In addition, it is known that the important role of N/OFQ on the signal pathways via chemical mediators involved in the symptoms of neuropathic pain or inflammatory pain. Thus, proinflammatory cytokines such as tumor necrosis factor-α (TNF-α), interleukin-1β (IL-1β), interleukin-6β (IL-6β),[10a–c] and monoamines such as norepinephrine (NE, or noradrenaline)[10d–j] and tachykinins[10k–n] work as neurotransmitters of pain signal in the DRG, peripheral tissues including sciatic nerve, and/or spinal cord, that is, evoke, maintain or potentiate neuropathic pain or inflammation status. Also, the role of calcium channels for pain-related neurotransmitter releases or for neuropathic pain perception, and the overexpression of calcium channels in diabetic neuropathy model have been reported.[4f,10o,10p] However NOP receptor activation by N/OFQ inhibits messenger RNA (mRNA) expressions and/or releases of the mediators or neurotransmitters such as the proinflammatory cytokines,[11a] NE,[11b,11c] and tachykinins[11d] in the peripheral sensory nerves or other peripheral tissues, and/or spinal cord. Furthermore, N/OFQ in the DRG or spinal cord suppresses excitatory synaptic transmission of C-fiber and Aδ-fiber neurons, inhibits Ca^{2+} currents, and internalizes calcium channels[4f,11e–g] for blocking pain-sensation or pain-signal transmissions.

Supplementary, other neural roles of N/OFQ in the various tissues and organs have been reported. In the brain, N/OFQ showed reversal effect against stress- or opioid-induced analgesia and blocking effects against opioid- or other drug-addictions, while N/OFQ showed complex actions in various models in terms of pain-signal transmissions as its supraspinal effects.[7b,12a] Also, intravenously administered N/OFQ showed inhibitory effect on skin or dural vasodilation evoked by stimulation of trigeminal sensory nerve endings or C-fiber, which indicated the potentiality of NOP receptor for the treatments of inflammation or migraine.[12b,12c] In the airways, N/OFQ showed suppression effects on evoked tachykinin substance P release, bronchoconstriction, acid-induced C-fiber neuron activation, and cough.[12d,12e] Besides, centrally or peripherally administered N/OFQ showed its neural roles for the protection and maintenance of gastric mucosa.[12f]

Overall, these studies have shown that NOP receptor activation is a significant target for the treatment of neuropathic pain as well as acute pain or inflammation, although there has been no report for clinical candidate-drug of NOP receptor agonist as analgesic for now. Alternatively, we have investigated NOP receptor agonist to create systemically active analgesic for the treatment of neuropathic pain as drug-discovery approach, expecting its potential advantages over previous drugs in terms of effectiveness with no or minimized adverse-effects.[1]

Herein, the rational drug design, synthesis, and structure–activity relationship (SAR) studies of peripheral- and/or spinal cord-targeting novel NOP receptor agonist to identify systemically active analgesic for the treatment of neuropathic pain, especially against mechanical allodynia that is a major and common issue in the neuropathic pain states,[3c] and the discovery of NOP receptor agonist {1-[4-(2-{hexahydropyrrolo[3,4-*c*]pyrrol-2(1*H*)-yl}-1*H*-benzimidazol-1-yl)piperidin-1-yl]cyclooctyl}methanol (HPCOM) **1** (Fig. 1) as a potential new-class analgesic with its unique mechanisms of systemically potent analgesic activity and safe profiles are described in detail as significant findings. The insights for further NOP receptor agonist study are discussed as well.

2. Results and discussion

2.1. Synthesis

2.1.1. Synthetic strategy

In general, the retrosynthesis of **1** and its analogues, that is, 1,2-disubstituted benzimidazole derivatives that contain 1-(hydroxymethyl)cycloalkyl group or other converted group for this study is outlined in Scheme 1.[2a] The synthetic strategy including various chemoselective reactions for the analogues is different from the recently reported synthetic method for the different series of 1,2-disubstituted benzimidazole derivatives that contain 1-methylcyclooctyl group such as MCOPPB and its analogues developing for potent brain activity per os as NOP receptor-selective agonists.[2b]

Thus, hydrophilic hydroxymethyl functional group of **2** was converted from the corresponding methoxycarbonyl group of **3** at a later stage of the total synthesis, and the various chemotypes of 2-substituted benzimidazole units were constructed from 1,2-phenylenediamine portion of **4**, respectively. Methyl 1-(4-aminopiperidin-1-yl)cycloalkanecarboxylate moiety at 1-postion of the 1,2-phenylenediamine derivatives **4**, that is, **5** was constructed from the corresponding α-amino-cycloalkyl acid methyl ester **7** via methyl 1-(4-oxopiperidin-1-yl)cycloalkanecarboxylate **6**, respectively.

2.1.2. Synthesis of 1 (HPCOM) and *N*-benzyl analogue 21

Indeed, the total synthesis of **1** was performed as follows (Schemes 2 and 3). At first, cyclooctane spiro-hydantoin **9** was prepared by Bucherer–Bergs synthesis[13] from cyclooctanone **8** with

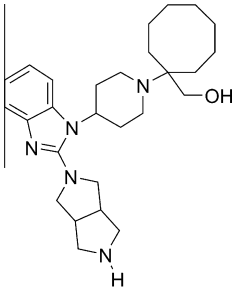

HPCOM, 1

Figure 1. Structure of novel systemically potent NOP receptor agonist {1-[4-(2-{hexahydropyrrolo[3,4-*c*]pyrrol-2(1*H*)-yl}-1*H*-benzimidazol-1-yl)piperidin-1-yl]-cyclooctyl}methanol **1** (HPCOM).

[†] The following abbreviations are in accordance with Nomenclature Committee of the International Union of Pharmacology (NC-IUPHAR): NOP receptor, N/OFQ peptide receptor (or opioid-receptor-like-1 receptor, ORL1 receptor); MOP receptor, μ-opioid peptide receptor; KOP receptor, κ-opioid peptide receptor; DOP receptor, δ-opioid peptide receptor; hNOP, hMOP, hKOP, and hDOP receptors, human NOP, human MOP, human KOP, and human DOP receptors, respectively.

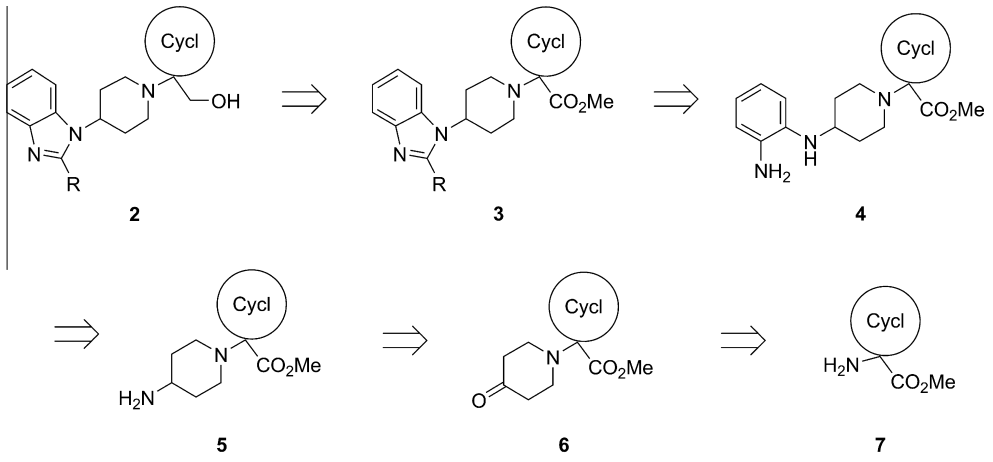

Cycl: cycloalkyl; R: alkyl or aryl.

Scheme 1. Retrosynthesis of (1-{4-[1*H*-(2-substituted benzimidazol)-1-yl]piperidin-1-yl}cyclooctyl)methanol analogues **2** from α-amino-cycloalkycarboxylic acid methyl ester **7**.

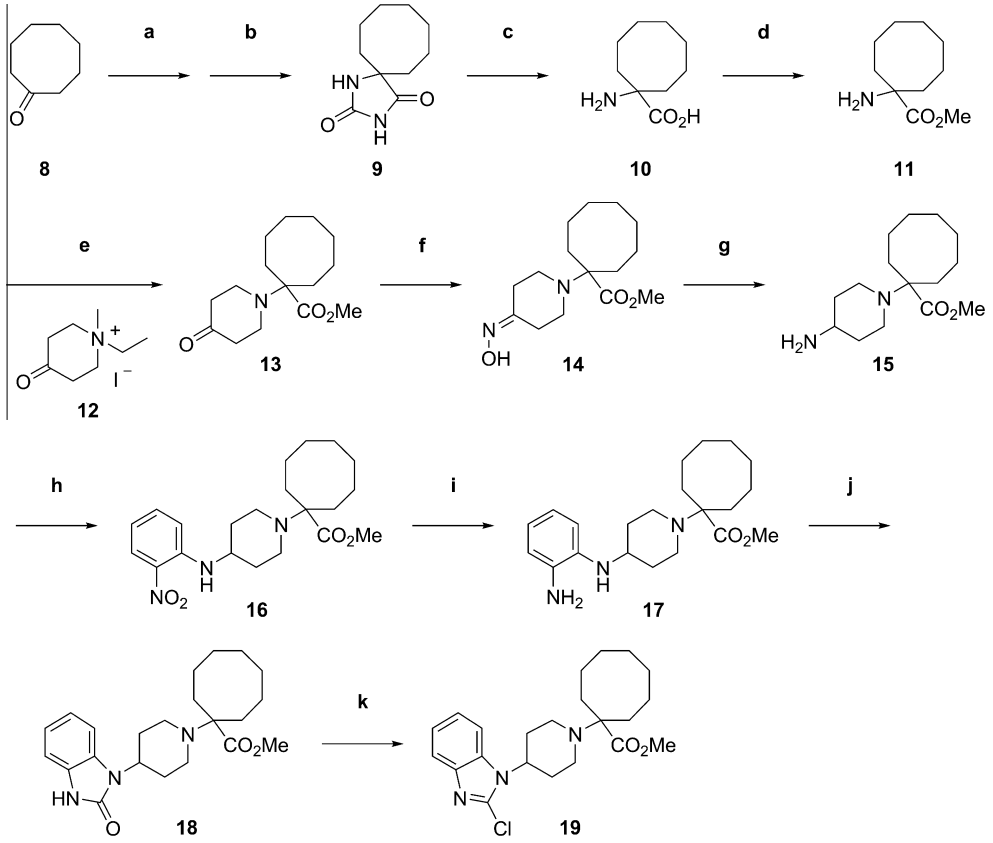

Scheme 2. Synthesis of key intermediates **17** and **19**. Reagents and conditions: (a) $(NH_4)_2CO_3$, KCN, EtOH/H_2O, 60 °C; (b) concd HCl, 0 °C; (c) 3 N NaOH, reflux; then adjusted to pH 6, 0 °C; (d) dry HCl (gas)/MeOH, 0 °C to reflux; (e) K_2CO_3, MeOH/H_2O, reflux; (f) NH_2OH·HCl, AcONa, MeOH; (g) H_2, PtO_2, 10% HCl/MeOH; (h) 1-fluoro-2-nitrobenzene, K_2CO_3, CH_3CN, reflux; (i) Zn (powder), NH_4Cl, MeOH/THF/H_2O; (j) CDI, THF, 0 °C to rt; (k) $POCl_3$, 110 °C to reflux.

ammonium carbonate and potassium cyanide, then hydrolyzed with aqueous NaOH to convert into the corresponding α-amino-cyclooctyl acid **10**, followed by methyl esterification in acidic condition. The obtained methyl 1-aminocyclooctanecarboxylate **11** was treated with 1-ethyl-1-methyl-4-oxopiperidinium iodide **12**, that was prepared from 1-methyl-4-piperidone and EtI, for Hofmann elimination/intramolecular cyclization to construct piperidone-skeleton **13**.[14] The oxo group of the piperidone derivative **13** was treated with hydroxylamine to convert into oxime **14**, followed by hydrogenation with PtO_2 in acidic condition[15] to generate primary amine **15**. The primary amino moiety of **15** was coupled with *o*-fluoro-nitrobenzene[16] to afford **16**. After the

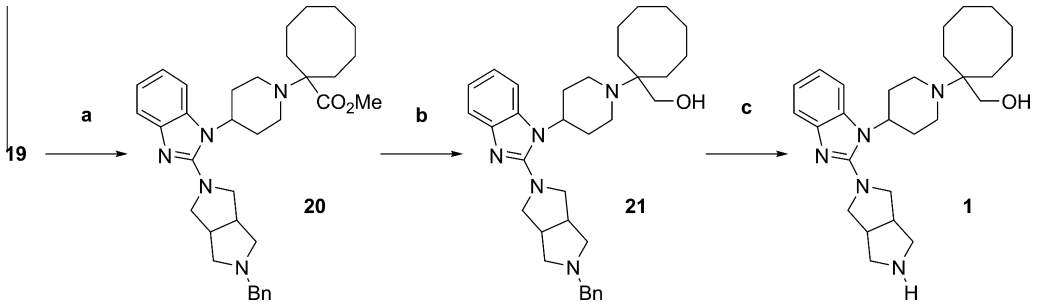

Scheme 3. Synthesis of {1-[4-(2-{hexahydropyrrolo[3,4-*c*]pyrrol-2(1*H*)-yl}-1*H*-benzimidazol-1-yl)piperidin-1-yl]cyclooctyl}methanol **1** (HPCOM) via *N*-benzyl derivative **21**. Reagents and conditions: (a) 2-benzyloctahydropyrrolo[3,4-*c*]pyrrole, MeOH, sealed-tube, 120 °C; (b) LAH, Et_2O, 0 °C to rt; (c) H_2, $Pd(OH)_2$, MeOH.

nitrobenzene moiety of **16** was converted into aniline by reduction with zinc[17] to give **17**, the 1,2-phenylenediamine portion was carbonylated with 1,1′-carbodiimidazole (CDI) to afford the corresponding 1*H*-benzimidazol-2(3*H*)-one **18**. In succession, the oxo group of 1*H*-benzimidazol-2(3*H*)-one **18** was converted into chloride with $POCl_3$ to afford 2-chloro-1*H*-benzimidazole **19**. Then the chloride portion of **19** was substituted with 2-benzyloctahydropyrrolo[3,4-*c*]pyrrole[18] to afford 1,2-disubstituted benzimidazole methyl ester **20**. The methoxycarbonyl group of **20** was exclusively converted into hydroxymethyl group by reduction with lithium aluminum hydride (LAH) to give the corresponding *N*-benzyl methyl alcohol analogue **21** in good yield. Finally, the *N*-benzyl portion of the 1,2-disubstituted benzimidazole derivative **21** was deprotected by hydrogenolysis with $Pd(OH)_2$ to afford the requisite final compound **1** as a sole product in good yield. As a supplemental synthetic study, LAH reduction with AcOEt–H_2O quenching procedure on N-unprotected methyl 1-[4-(2-{hexahydropyrrolo[3,4-*c*]pyrrol-2(1*H*)-yl}-1*H*-benzimidazol-1-yl)piperidin-1-yl]cyclooctanecarboxylate was tried as the final step for the synthesis of **1** instead of the above route, which yielded a complex mixture probably derived from **1** itself with aluminum, and it was hard to convert the mixture into pure product **1** by potassium fluoride or aqueous $NaHCO_3$ treatment.

On the other hand, the above intermediates **17** and **19** were also used for other analogue syntheses as follows (Schemes 4–6).

2.1.3. Synthesis of 2-(cycloalkylamino)benzimidazole analogues 23, 27, and 31, and ester analogue 22

As other 2-cycloalkylamino-substituted benzimidazole analogues that contain 1-(hydroxymethyl)cyclooctyl portion, **23**, **27**, and **31** were prepared. Thus, the above intermediate **19** was coupled with the various secondary amines in the same manner mentioned above to afford 1,2-disubstituted benzimidazole methyl esters **22**, **24**, and **28**, respectively. In case of 2-(*N*-methylpiperazinyl)benzimidazole derivative, that is, 1-(methoxycarbonyl)cyclooctyl analogue **22**, the methoxycarbonyl group was reduced with LAH as the last step to afford the corresponding methyl alcohol analogue **23** (Scheme 4). In case of 2-(*NH*-piperazinyl)benzimidazole derivatives **24** and **28**, through protection of the respective *NH*-portion as *N*-benzylamino group, the resulting methyl ester derivatives **25** and **29** were converted to methyl alcohol derivatives **26** and **30** by reduction with LAH, respectively, and then the *N*-benzylamino groups were deprotected by hydrogenolysis in the same way of the preparation of **1**, to afford *NH*-piperazine derivatives **27** and **31**, respectively (Scheme 5).

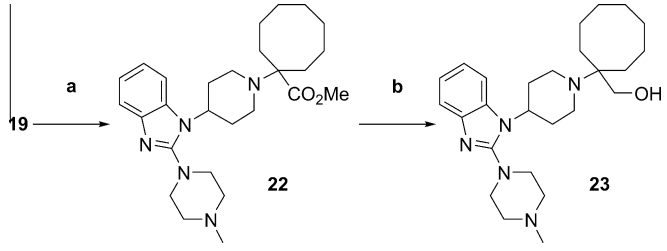

Scheme 4. Synthesis of (1-{4-[2-(4-methylpiperazin-1-yl)-1*H*-benzimidazol-1-yl]piperidin-1-yl}cyclooctyl)methanol **23** via methyl ester derivative **22**. Reagents and conditions: (a) 1-methylpiperazine, 110 °C; (b) LAH, THF, 0 °C to rt.

2.1.4. Synthesis of 2-arylbenzimidazole analogues 33, 35, and 45

For the preparation of 2-aryl-substituted benzimidazole analogues containing 1-(hydroxymethyl)cyclooctyl portion, the respective benzimidazole skeletons were constructed from the 1-substituted 1,2-phenylenediamine intermediate **17** in two ways: (i) oxidative condensation of the 1,2-phenylenediamine **17** with arylaldehyde promoted by $Cu(OAc)_2$ to obtain **32**;[19] and (ii) amidation of the 1,2-phenylenediamine **17** with arylcarboxylic acid and subsequent intramolecular dehydrative condensation of the amide and amino portions with $POCl_3$ to obtain **34**. These 2-arylbenzimidazole methyl ester derivatives **32** and **34** were reduced with LAH to generate the corresponding methyl alcohol derivatives **33** and **35**, respectively (Scheme 6).

Besides, as the cycloalkyl ring size variation on the piperidine ring for the series of analogues, 1-(hydroxymethyl)cyclohexyl-type benzimidazole analogue **45** was synthesized from α-amino-cyclohexylcarboxylic acid **36** as a raw material in the same manner for the preparation of the corresponding 1-(hydroxymethyl)cyclooctyl-type benzimidazole analogue **35** described above (Scheme 7).

2.1.5. Synthesis of carboxylic acid analogue 46 and 1*H*-benzimidazol-2(3*H*)-one analogue 47

Furthermore, as other hydrophilic group-substituted analogue, 1-carboxycyclooctyl analogue **46** was synthesized by alkalic hydrolysis of the corresponding methyl ester derivative **22**. Also, 1-(hydroxymethyl)cyclooctyl-type 1*H*-benzimidazol-2(3*H*)-one derivative **47** was prepared from the above corresponding methyl ester **18** by LAH reduction (Scheme 8).

2.1.6. The purities of the analogues and 2D NMR correlations of 1

All of these structurally novel 1,2-disubstituted benzimidazole derivatives **1**, **21**–**23**, **27**, **31**, **33**, **35**, **45**, and **47** were converted into tri- or dihydrochloride using HCl in MeOH, respectively. The purities of the hydrochlorides of **1**, **21**–**23**, **27**, **31**, **35**, **45**, and **47**, and salt free compound **46** were confirmed by elementary analysis to be within ±0.4% of calculated values, respectively, and the exact masses of **33** and **46** were confirmed by HRMS-FAB measurement, respectively (see Section 4). These compounds were used for SAR studies with pharmacological and/or pharmacokinetic evaluations.

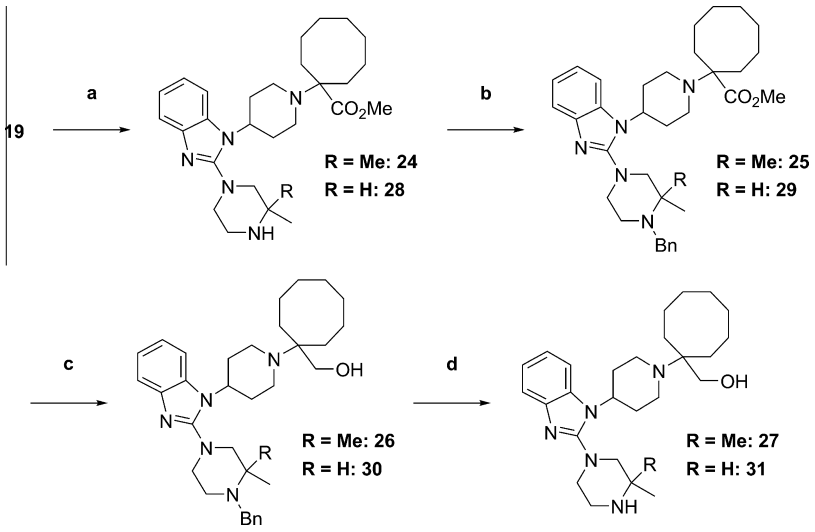

Scheme 5. Synthesis of (1-{4-[2-(piperazin-1-yl)-1*H*-benzimidazol-1-yl]piperidin-1-yl}cyclooctyl)methanol derivatives **27** and **31**. Reagents and conditions: (a) 2,2-dimethyl piperazine for **24**, or 2-methylpiperazine for **28**, MeOH, sealed-tube, 120 °C; (b) benzyl bromide, K_2CO_3, toluene, reflux; (c) LAH, THF, 0 °C to rt; (d) H_2, $Pd(OH)_2$, MeOH for **27**, or H_2, 10% Pd/C, HCl/MeOH for **31**.

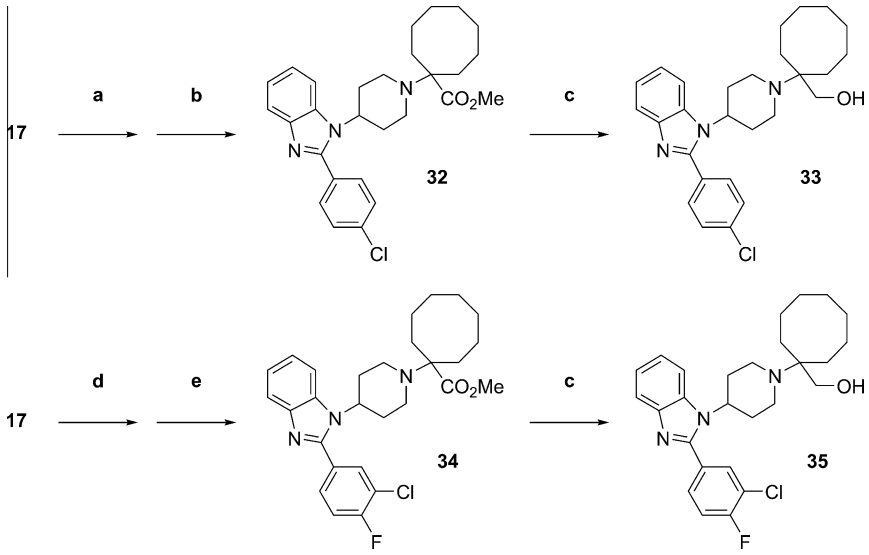

Scheme 6. Synthesis of {1-[4-(2-aryl-1*H*-benzimidazol-1-yl)piperidin-1-yl]cyclooctyl}methanol derivatives **33** and **35**. Reagents and conditions: (a) 4-chlorobenzaldehyde, EtOH, reflux; (b) $Cu(OAc)_2{\cdot}H_2O$, PhH; (c) LAH, THF or Et_2O/THF, 0 °C to rt; (d) 3-chloro-4-fluorobenzoic acid, WSCI, THF, −20 °C to rt; (e) $POCl_3$, 110 °C to reflux.

As well, full assignments of ^1H and ^1C NMR data, and key ^1H–^1H COSY, HMBC, and NOESY correlations for HCl salt of **1** were established as shown in Table 1 and Figure 2, respectively (see also Section 4).

2.2. Drug design strategy for systemically potent NOP receptor agonist as analgesic against neuropathic pain

As mentioned, NOP receptor activation by peripheral or spinal N/OFQ has exhibited various analgesic effects in animal models and inhibitory effects on pain-signal transmissions, while complex supraspinal actions of N/OFQ for pain-signal transmissions have been reported. Alternatively, peripheral neuropathy is a major or common cause of neuropathic pain disorder. Consequently, for the discovery study to identify systemically effective new-class analgesic for the treatment of neuropathic pain, it would be significant to design potent and selective NOP receptor agonist directing high or sufficient concentration levels in the peripheral and/or spinal cord with relatively low brain selectivity utilizing the property of blood–brain barrier (BBB), the tight junction network of capillary endothelial cell. In particular, highly hydrophilic (far lowly lipophilic) and/or large compound is prevented from (or limited to a certain level for) the passive diffusion across the lipid bilayer membrane of the endothelial cell unless appropriate transport-system exists to the uptake of the compound into the brain, hence the investigation of appropriately highly hydrophilic molecule, for example, the molecule bearing multisite hydrogen-bonding functional groups as hydrophilic moieties and having sufficiently low lipophilicity for the whole molecular-structure, would be expectable to acquire and/or maintain the desired pharmacokinetic character such as high plasma exposure with plasma-to-brain selectivity in the subcutaneous (systemic) administration condition. As well, high binding- and functional-selectivity of NOP receptor over classical opioid peptide receptors is important to prevent or minimize adverse-effects derived from the CNS actions of the classical opioid peptide receptors.

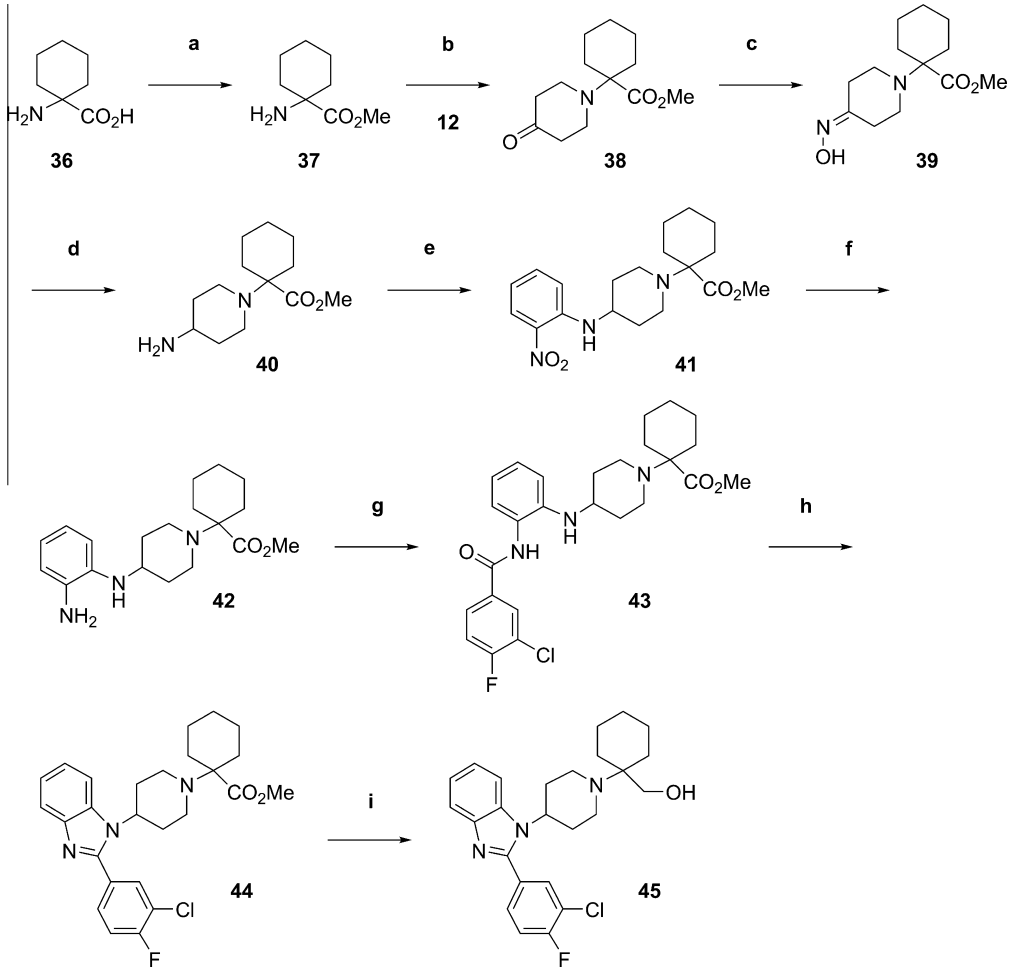

Scheme 7. Synthesis of (1-{4-[2-(3-chloro-4-fluorophenyl)-1*H*-benzimidazol-1-yl]piperidin-1-yl}cyclohexyl)methanol **45**. Reagents and conditions: (a) $SOCl_2$, MeOH, −10 °C to rt; (b) K_2CO_3, MeOH/H_2O, reflux to rt; (c) NH_2OH·HCl, AcONa, MeOH; (d) H_2, PtO_2, 10% HCl/MeOH; (e) 1-fluoro-2-nitrobenzene, K_2CO_3, CH_3CN, reflux; (f) Zn (powder), NH_4Cl, MeOH/THF/H_2O; (g) 3-chloro-4-fluorobenzoic acid, WSCI, THF, −20 °C to rt; (h) $POCl_3$, 110 °C to reflux; (i) LAH, THF, 0 °C to rt.

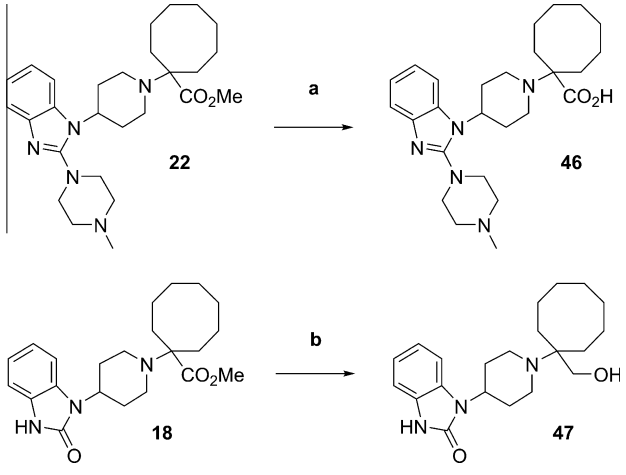

Scheme 8. Synthesis of compounds **46** and **47**. Reagents and conditions: (a) 2 N NaOH, EtOH, reflux; then adjusted to pH 6, 0 °C; (b) LAH, THF, 0 °C to rt.

Actually, drug design, synthesis, and SAR of novel NOP receptor agonist with 1,2-substituted benzimidazole derivatives to identify systemically potent new-class analgesic were investigated for (i) potent binding affinity and functional activity, and high selectivity for NOP receptor in vitro, (ii) robust metabolic stability, (iii) high peripheral- and/or spinal cord-exposure with high plasma-to-brain ratio in vivo, and (iv) significant analgesic activity against mechanical allodynia in CCI-induced peripheral nerve injury model rats in the subcutaneous administration condition. The significant and attractive findings of this study are shown in the present article step by step.

On the other hand, by contrast, non-peptide NOP receptor agonists have been reported by us, that is, MCOPPB,[1,2b–d] and by other research groups such as Ro 64-6198[20a] and SCH 221510,[20b] which were conducted for brain-active antianxiety drug. In our distinctive drug design and SAR study with the different series of 1,2-disubstituted benzimidazole analogues for new-class anxiolytic that has advantageous profiles over classical anxiolytic such as diazepam in terms of side-effects, the desired novel NOP receptor agonist such as MCOPPB required (i) potent and selective in vitro NOP receptor activity, and (ii) distinctive and appropriate molecular property to achieve orally potent brain activity via permeation in the intestine followed by penetration through BBB in the oral administration condition.[1,2b,2c] While the present and MCOPPB studies were performed with respective drug discovery target-oriented strategy, complementary SARs including MCOPPB analogues for in vitro and pharmacokinetic viewpoints are discussed to get better or comprehensive understanding of the present study as well.

Table 1
^{1}H and ^{13}C NMR spectral data for HCl salt of **1** in CD_3OD[a]

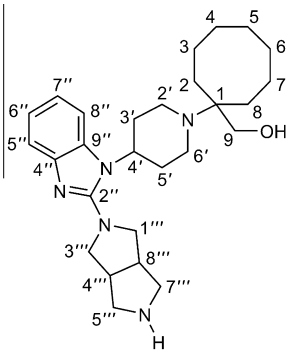

Portion of **1**	Position[b]	δ_H (multiplicity, J in Hz)[c]	δ_C (multiplicity)[d]
1-(Hydroxymethyl)cyclooctyl	1		75.8 (s)
	2/8	2.36 (t, 12.35), 1.76 (overlap)[e]	28.8 (t)
	3/7	1.85 (m), 1.72 (overlap)[e]	25.4 (t)
	4/6	1.76 (overlap),[e] 1.40 (m)	30.1 (t)
	5	1.75 (overlap),[e] 1.46 (m)	27.7 (t)
	9	3.74 (s)[f]	63.1 (t)
Piperidinyl	2′/6′	3.81 (d, 10.82), 3.73 (overlap)[f]	48.3 (t)
	3′/5′	2.98 (m), 2.30 (d, 12.97)	29.1 (t)
	4′	5.09 (br t, 12.55)	54.2 (d)
1*H*-Benzimidazol-1-yl	2″		154.4 (s)
	4″		134.7 (s)
	5″	7.51 (dd, 5.70, 2.14)	115.5 (d)
	6″	7.36 (overlap)[g]	126.3 (d)
	7″	7.35 (overlap)[g]	125.4 (d)
	8″	7.97 (m)	115.2 (d)
	9″		132.1 (s)
Hexahydropyrrolo[3,4-*c*]pyrrol-2(1*H*)-yl	1‴/3‴	4.00 (d, 8.44), 3.93 (m)	56.5 (t)
	4‴/8‴	3.39 (br s)	44.3 (d)
	5‴/7‴	3.61 (dd, 12.26, 7.36), 3.54 (dd, 12.16, 3.27)	51.3 (t)

[a] See also Figure 2 and Section 4.
[b] Atom position in the respective portion of **1**.
[c] Measured at 600 MHz.
[d] Measured at 150 MHz; Multiplicity by proton interaction.
[e–g] Overlapped with each other.

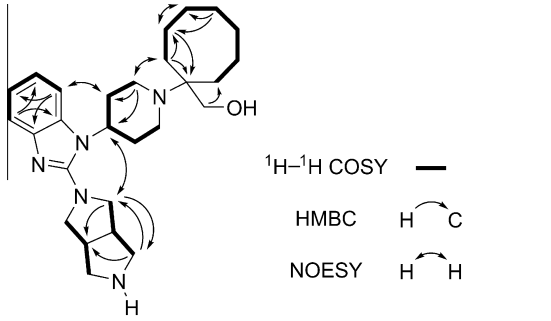

1

Figure 2. Key ^{1}H–^{1}H COSY, HMBC, and NOESY correlations for HCl salt of **1**.

2.3. Structure–activity relationships of NOP receptor agonists

2.3.1. In vitro activity and selectivity for hNOP receptor

As the first step of the present study, design, synthesis, and in vitro SAR studies of 1,2-disubstituted benzimidazole analogues were performed for potent binding affinity and biological functional activity for the recombinant human NOP (hNOP) receptor expressed in HEK (human embryonic kidney)-293 cells, and for high selectivity to hNOP receptor against human classical opioid peptide receptors such as human MOP receptor (hMOP receptor), human KOP receptor (hKOP receptor), and human DOP receptor (hDOP receptor) expressed in Chinese hamster ovary (CHO)-K1 cells, HEK-293 cells, and HEK-293 cells, respectively: (i) the receptor–ligand binding assays for K_i value[21] with respective radiolabeled ligands such as [^{3}H]N/OFQ for hNOP receptor, [^{3}H]DAMGO for hMOP receptor, [^{3}H]enadoline for hKOP receptor, [^{3}H]DPDPE for hDOP receptor, and (ii) the functional assays using [^{35}S]guanosine 5′-(γ-thiotriphosphate) ([^{35}S]GTPγS) binding to α-unit of G-protein in response to the receptor–ligand binding for EC_{50} (potency) value and E_{max} (efficacy) value (see Section 4).

Actually, introduction of various hydrophilic- and/or polar-moieties at plural sites and conversion of various characteristic substituents for 2-substituted 1-(1-cycloalkyl-4-piperidinyl)-1*H*-benzimidazole analogues were significant in this and later steps. The results of the in vitro SAR study for various 1,2-disubstituted benzimidazole analogues are shown in Table 2.

First, the SAR study of 1-substituent portion for benzimidazole derivatives led to encouraging results for performing further analogue development. Thus, *N*-methyl-1-piperazine analogues, 1-(methoxycarbonyl)cyclooctyl analogue **22**, 1-(hydroxymethyl)-cyclooctyl analogue **23**, and 1-carboxycyclooctyl analogue **46** were designed and investigated for identifying appropriate structure as potent and selective NOP receptor agonist that contained hydrophilic- and/or polar-functionality, also considering the desired pharmacokinetic property of this study (see later step). Among

Table 2
Structure–activity relationships of in vitro binding affinities and functional activities to human recombinant NOP receptor and classical opioid peptide receptors for 1,2-disubstituted benzimidazole analogues

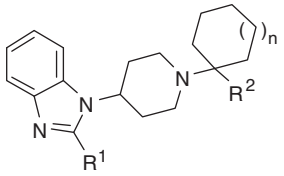

Compound				Binding affinity K_i (nM)[a]				Functional activity [^{35}S]GTPγS EC_{50} (nM)[b] E_{max} (%)[c]		
No.	R^1	R^2	*n*	hNOP	hMOP	hKOP	hDOP	hNOP	hMOP	hKOP
1	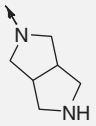	CH_2OH	3	1.438	201	>577	>5000	12 144%	3500 14%	ND[d] 22%
21	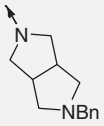	CH_2OH	3	6.56	128	39.0	258	NT[e]	NT	NT
22	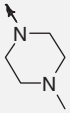	CO_2Me	3	80.5	>450	>570	312	NT	NT	NT
23	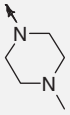	CH_2OH	3	4.29	229	333	679	17 104%	ND 13%	18 34%
27		CH_2OH	3	4.54	>450	387	>500	23 132%	ND 2%	ND 14%
31		CH_2OH	3	0.96	>450	275	>500	38 151%	1772 15%	366 18%
33	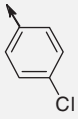	CH_2OH	3	0.15	178	>570	205	9.1 161%	>10,000 30%	ND 1%
35	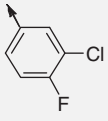	CH_2OH	3	0.73	302	NT	NT	8.9 140%	1219 12%	NT
45	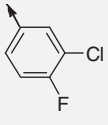	CH_2OH	1	4.29	>450	NT	NT	53 106%	ND 6%	NT
46	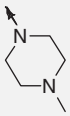	CO_2H	3	>250	>450	>570	NT	NT	NT	NT

Table 2 (*continued*)

Compound				Binding affinity K_i (nM)[a]				Functional activity [^{35}S]GTPγS EC_{50} (nM)[b] E_{max} (%)[c]		
No.	R^1	R^2	*n*	hNOP	hMOP	hKOP	hDOP	hNOP	hMOP	hKOP
47	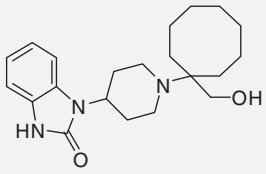			4.29	16.0	239	>5000	37 136%	144 13%	194 50%
	N/OFQ			0.39	>1000[f]	>1000[f]	>1000[f]	1.5 100%	NT	NT

[a] K_i values for these compounds were measured by displacement of [^{3}H]N/OFQ binding to hNOP receptor expressed in HEK-293 cells, [^{3}H]DAMGO binding to hMOP receptor expressed in CHO-K1 cells, [^{3}H]enadoline binding to hKOP receptor expressed in HEK-293 cells, and [^{3}H]DPDPE binding to hDOP receptor expressed in CHO-K1 cells. $K_i = IC_{50}/(1+[\text{radioligand}]/K_D)$. Radioligands: [^{3}H]N/OFQ as hNOP receptor agonist, concentration 0.4 nM, K_D = 0.135 nM; [^{3}H]DAMGO as hMOP receptor agonist, concentration 1.0 nM, K_D = 0.821 nM; [^{3}H]enadoline as hKOP receptor agonist, concentration 0.5 nM, K_D = 0.683 nM; [^{3}H]DPDPE as hDOP receptor agonist, concentration 2.0 nM, K_D = 2.00 nM.

[b] EC_{50} values for these compounds were determined by induction of the binding of [^{35}S]GTPγS to α-unit of G-protein due to binding of the compounds to hNOP receptor expressed in HEK-293 cells, hMOP receptor expressed in CHO-K1 cells, hKOP receptor expressed in HEK-293 cells, and hDOP receptor expressed in CHO-K1 cells.

[c] E_{max} (efficacy) value was the maximal response calculated as the percentage of the maximal response produced by each control (N/OFQ, DAMGO, enadoline, and DPDPE).

[d] ND, not detected.

[e] NT, not tested.

[f] Data from Ref. 22.

them, the 1-(hydroxymethyl)cyclooctyl analogue **23** exhibited potent NOP receptor binding affinity with high selectivity to hNOP receptor against human classical opioid peptide receptors, that is, the K_i values were 4.29 nM (hNOP), 229 nM (hMOP), 333 nM (hKOP), and 679 nM (hDOP). In contrast, other analogues showed much less K_i values to hNOP receptor, that is, the K_i values of the corresponding 1-methoxycarbonyl analogue **22** were 80.5 nM (hNOP), and the K_i values of the corresponding 1-carboxy analogue **46** were >250 nM (hNOP). Furthermore, **23** exhibited selective hNOP receptor agonist activity (shown below). These results suggested that 1-(hydroxymethyl)cyclooctyl group was promising for further analogue development to identify potent and selective NOP receptor agonist.

Second, the design and SAR study was subsequently performed for hydroxymethyl group-containing analogues focusing on the 2-substituent effect of benzimidazole core, that is, 1-[1-(hydroxymethyl)cycloalkyl]piperidine analogues were investigated in vitro. In general, various chemotypes 2-substituted benzimidazole analogues of 1-[1-(hydroxymethyl)cyclooctyl]piperidine derivatives, namely, 2-cycloaminoalkyl analogues **1**, **21**, **23**, **27**, and **31**, 2-aryl analogues **33** and **35**, and 2-oxo analogue, that is, 1*H*-benzimidazol-2(3*H*)-one analogue **47**, exhibited potent binding affinities to hNOP receptor, that is, the K_i values were 0.15–6.56 nM. Among these comparison, the rank of orders of the binding affinities (K_i values) for the 2-substituents is 4′-Cl-phenyl (**33**), 3′-Cl-4′-F-phenyl (**35**) > *NH*-hexahydropyrrolo[3,4-*c*]pyrrol-2′-yl (**1**), 3′-Me-piperazinyl (**31**) > *N*-Me-piperazinyl (**23**), 3′,3′-di-Me-piperazinyl (**27**), 2-oxo (**47**) ≫ *N*-benzylhexahydropyrrolo[3,4-*c*]pyrrol-2′-yl (**21**), which shows high effectiveness of mono- or fused-cyclic 2-substituents for the potency of 1-(hydroxymethyl)cyclooctyl-type 1,2-disubstituted benzimidazole analogue except *N*-benzylhexahydropyrrolo[3,4-*c*]pyrrol-2′-yl substituent (**21**) that is bulkier than the others. Significantly, 2-(cycloamino or aryl)-1*H*-benzimidazole analogues of 1-[1-(hydroxymethyl)-cycloalkyl derivatives **1**, **23**, **27**, **31**, **33**, **35**, and **45** showed high selectivities for the hNOP receptor binding affinity (K_i) against human classical opioid peptide receptors, that is, 53- to beyond 3400-fold hNOP receptor selectivity, but *N*-benzylhexahydropyrrolo[3,4-*c*]pyrrol-2'-yl analogue **21** and 1*H*-benzimidazol-2(3*H*)-one analogue **47** showed low selectivities, which indicate the advantage of appropriate range of bulkiness as 2-substituent for hNOP receptor selectivity (see later further discussion). As well, the hydroxymethyl-type 2-substitued benzimidazole analogues **1**, **23**, **27**, **31**, **33**, **35**, and **45** exhibited potent functional activities for [^{35}S]GTPγS binding via the analogue–hNOP receptor binding, that is, the EC_{50} values were 8.9–53 nM, and the respective maximal effects were greater than that of N/OFQ, namely, these were hNOP receptor full agonists. Furthermore, the hydroxymethyl-type 2-substitued benzimidazole analogues displayed highly selective or specific hNOP receptor functional activities over hMOP (**1**, **23**, **27**, **31**, **33**, **35**, and **45**) and hKOP receptors (**1**, **23**, **27**, **31**, and **33**). Significantly, the respective maximal effects of the hNOP receptor agonists to the human classical opioid peptide receptors such as hMOP and hKOP receptors were of partial or none. As well, the binding affinities of hDOP receptor for **1**, **23**, **27**, **31**, and **33** were extremely low. For the ring size comparison of cycloalkyl group on piperidine portion in the 1-substituent of benzimidazole core, 2-(3-chloro-4-fluorophenyl)-1*H*-benzimidazole analogues were investigated, thus, the cyclooctyl analogue **35** showed sixfold potent hNOP receptor binding affinity (K_i) and functional activity (EC_{50}) than those of the corresponding cyclohexyl analogue **45**.

As the mostly significant results through the present SAR study in vitro, **1** demonstrated potent and highly selective/specific activity for hNOP receptor against human classical opioid peptide receptors similar to the endogenous ligand N/OFQ.[22] Thus, (i) the K_i values of **1** for the binding affinities were 1.438 nM (hNOP), 201 nM (hMOP), >577 nM (hKOP), and >5000 nM (hDOP), that is, the binding selectivities of hNOP receptor binding against human classical opioid peptide receptors were 140-fold over hMOP receptor, >400-fold over hKOP receptor, and >3470-fold over hDOP receptor, respectively; and (ii) relative to the high functional potency (EC_{50} = 12 nM) and high maximal efficacy (E_{max} = 144%) of **1** for hNOP receptor, the functional potency for hMOP or hKOP receptors was very weak or not detected and the respective efficacy was of partial or little, that is, EC_{50} = 3500 nM, E_{max} = 14% for hMOP receptor, EC_{50} = not detected, E_{max} = 22% for hKOP receptor, respectively. Notably, **1** was designed as (i) the lowest-lipophilic compound among 1,2-disubstituted benzimidazole analogues in our study and (ii) the molecule bearing multisite hydrogen-bonding functional groups, which were significant properties as shown in the later steps.

Besides, based on the present study, the SAR studies of MCOPPB analogues that were designed for their own purpose-oriented strategy and of our other benzimidazole analogues were useful to seek further and comprehensive pharmacophoric insights in terms of in vitro interaction between hNOP receptor and 1,2-disubstituted benzimidazole analogue as hNOP receptor agonist. The present and MCOPPB analogues which developed for analgesic and for anxiolytic, respectively, bear 1*H*-benzimidazol-1-yl-piperidine framework that has been found out to be a unit of NOP receptor agonists in our SAR studies including several library-compound screening studies as well.

First, compared with the 1-substituent of cycloalkyl group on piperidine ring in the 1-substituent portion of benzimidazole core, the present 1-(hydroxymethyl)cyclooctyl-type analogues exhibited higher hNOP receptor selectivity against human classical opioid peptide receptors while the 1-methylcyclooctyl-type MCOPPB analogues (2-substituted 1-[1-(1-methylcyclooctyl)piperidin-4-yl]-1*H*-benzimidazole derivatives) exhibited somewhat greater hNOP receptor binding affinities, as general tendency for their in vitro SARs.[2b] For example, 1-(hydroxymethyl)cyclooctyl-type 3′-Cl-4′-F-phenyl analogue **35** was more selective and less potent hNOP receptor binding affinity than the corresponding 1-methylcyclooctyl-type 3′-Cl-4′-F-phenyl analogue, that is, the binding affinities of **35** were K_i = 0.73 nM for hNOP receptor and K_i = 302 nM for hMOP receptor, and those of the corresponding 1-methylcyclooctyl-type analogue were K_i = 0.22 nM for hNOP receptor and K_i = 45 nM for hMOP receptor.[2b] Compared with the SAR for (1-substituted cyclooctyl)-type *N*-methyl-1-piperazine analogues **22**, **23**, and **46** mentioned already, the corresponding various (1-substituted cycloalkyl)-type *N*-methyl-1-piperazine analogues (namely, 1-[1-(1-substituted cycloheptyl)piperidin-4-yl]-2-(4-methylpiperazin-1-yl)-1*H*-benzimidazole) gave supplemental information, that is, the respective K_i values for the binding affinities were 69.6 nM (hNOP), 78.4 nM (hMOP), 214 nM (hKOP), 25.5 nM (hDOP) for 1-acetylcycloheptyl analogue, 43.1 nM (hNOP), 45.5 nM (hMOP), 176 nM (hKOP), 327 nM (hDOP) for 1-(1-hydroxyethyl)cycloheptyl analogue, 16.4 nM (hNOP), 5.86 nM (hMOP), 51.4 nM (hKOP), 44.0 nM (hDOP) for 1-isopropylcycloheptyl analogue (further data not shown), which were generally much less potent and selective hNOP receptor binding affinities than those of the above 1-(hydroxymethyl)cyclooctyl-type analogue (**23**), for example, K_i = 4.29 nM (hNOP) for **23** (see above). The overall results for this portion indicated appropriate properties of pharmacophor: (i) 1-hydroxymethyl group (**23**) that has hydrogen bond donor (HBD) and hydrogen bond acceptor (HBA) functionalities was more effective for potent and selective hNOP receptor binding affinity than 1-methoxycarbonyl group (**22**) and 1-acetyl group that have only HBA functionality as well as 1-hydroxyethyl group that has HBD and HBA functionalities but somewhat bulkier group; and (ii) 1-isopropylcycloheptyl analogue group that is neutral and bulkier group without HBD and HBA functionalities showed less selectivity for hNOP receptor; however (iii) 1-carboxy group (**46**) that has HBD and HBA functionalities but has reduced pK_a relative to 1-hydroxymethyl group was unfavorable for the binding to hNOP receptor as well as human classical opioid peptide receptors.

In summary, small and neutral groups such as 1-hydroxymethyl and 1-methyl group of this portion were superior to others for potent hNOP receptor binding affinity, functional activity, and selectivity, furthermore, because of its HBD and HBA functionalities, 1-hydroxymethyl group would be more preferable for the hNOP receptor selective binding affinity against human classical opioid peptide receptors relative to 1-methyl group that has no such functionalities.

Second, the 2-substituent modifications of benzimidazole core were also significant in the present and MCOPPB analogue studies, respectively, and the in vitro profiles exhibited complementary or similarly between both series of analogues. Collectively, for this portion, (i) bicyclo- or monocyclo-functional groups were effective for potent and selective hNOP receptor activity in vitro, but rather bulkier analogue **21**, rather smaller analogue **47**, as well as 2-unsubstituted analogue, that is, 2-hydrogen-1*H*-benzimidazole derivative,[2b] showed less hNOP receptor affinity and/or selectivity as described, and (ii) neutral or basic functional groups as well as electron rich or poor groups were tolerated in common with both series. These results indicated similar appropriate or allowable ranges of this portion for steric bulkiness, sizes, shapes, and functional group properties in vitro for both series of analogues despite the difference between respective 1-substituents of cyclooctyl group.

As a conclusion of these studies, both series of 1,2-disubstituted benzimidazole analogues showed unique and significant SAR for the in vitro viewpoints, that is, the essential effects, requirements, scope, and limitation of the substituents of benzimidazole core for the activity, selectivity, and characteristic receptor interaction-modes as hNOP receptor agonist. Especially, the present study clarified that 1-(hydroxymethyl)cyclooctyl portion, together with appropriate 2-substituent portion of benzimidazole, was critical for the potent and higher selective or specific hNOP receptor binding affinity against the human classical opioid peptide receptors.

2.3.2. Pharmacokinetic studies

As the second step, pharmacokinetic studies of potent and selective NOP receptor agonist were performed to develop and identify high peripheral- and/or spinal cord-exposure structure, expecting systemic analgesic efficacy in vivo.

First, to get metabolically stable structure, half-lives in human liver microsome (HLM) were investigated for **1**, **23**, and **31** that had relatively low lipophilicity for the whole structure, respectively, among the hydroxymethyl functionality-containing analogues in this study. As shown in Table 3, the tendencies of the half-lives and the lipophilicity values at pH 7.4 as ACD log *D* calculated by ACD software (ACD log $D_{7.4}$) were indicated to be inverse for these analogues as expected, which were in line with the similar approaches to improve metabolic stability by reducing lipophilicity[2c,23] including recent reports for the other series of our NOP receptor agonists[2c] and statistical analysis with various compounds.[23c] Thus, depending on the property of 2-substituent of benzimidazole core, the lowest-lipophilic analogue **1** (ACD log $D_{7.4}$ = 1.08) apparently exhibited long-lasting half-life in HLM, that is, 45.6 min, and higher lipophilic analogues **23** (ACD log $D_{7.4}$ = 3.17) and **31** (ACD log $D_{7.4}$ = 3.09) relative to **1** showed shorter half-life, that is, 9.5 min and 19.7 min, respectively.

In our metabolite study for a couple of 1-methylcyclooctyl-type 1,2-disubstituted benzimidazole analogues in rat liver microsome by HPLC–MS/MS analysis, the major metabolites were hydroxylated-forms. The hydroxylation occurred at several sites on the cyclooctyl ring portion whereas did not occur at the 1-methyl group portion of the 1-methylcyclooctyl moiety (further data not shown). Assuming that the major metabolic reaction occurred at similar site(s) of the present 1-(hydroxymethyl)cyclooctyl-type 1,2-disubstituted benzimidazole analogues in HLM, that is, at the corresponding cyclooctyl ring portion, the property of the 2-substituent such as lipophilicity would possibly contribute to ease of the metabolic reaction that is potentially related to the instability of the analogues in HLM, although other potential metabolic-reaction-site, for example, the methyl portion in the 2-substituent for **23** or **31**, might also contribute to the shorten half-life. As mentioned, the inverse relationship between half-life and ACD log $D_{7.4}$ value was indicated for each series of analogues, that is, the present or MCOPPB analogues, which was related to the property of respective 2-substituent of benzimidazole core. Actually, the longest half-life was achieved by the lowest-lipophilic analogue in each series, that is, **1** among 1-(hydroxymethyl)cyclooctyl group-

Table 3
SAR of metabolic stabilities (half-lives in human liver microsome) versus lipophilicities, with other physicochemical properties for 1-(hydroxymethyl)cyclooctyl-type 1,2-disubstituted benzimidazole analogues

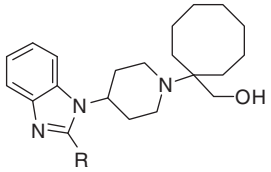

Compound		Half-life[a] (HLM) (min)	Physicochemical properties			
No.	R		Lipophilicity[b] ACD log $D_{7.4}$	Size M_W	HBD Number	HBA Number
1	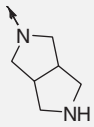	45.6	1.08	451.65	2	5
23	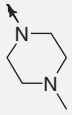	9.5	3.17	439.64	1	5
31		19.7	3.09	439.64	2	5

[a] Half-lives of these compounds in human liver microsome were measured by HPLC/MS/MS.
[b] Predicted by ACD/Laboratories 9.0.

containing 1,2-disubstituted benzimidazole analogues, and MCOPPB among 1-methylcyclooctyl group-containing 1,2-disubstituted benzimidazole analogues. However, MCOPPB showed longer half-life (123.8 min) than that of **1** in HLM, which was contrary to the relation of their lipophilicity for the whole structure. Therefore, the degree of lipophilicity derived from the 2-substituent character seemed to be reflected on the molecular half-life on condition that the structural feature of the other portion of the molecule was the same. The difference of half-lives between both series of analogues might be due to the differential degrees of reactivity (or affinity) for metabolic enzymes and/or other (e.g., secondary) metabolic reaction derived from their distinctive structural features, specifically, 1-(hydroxymethyl) and 1-methyl groups at the cyclooctyl portion, respectively. In our studies, lipophilicity estimation has been one of effective ways to design or predict metabolically stable NOP receptor agonist; in addition, it would be important to consider other factors that might affect the degree of metabolic stability such as shape, acidity, hydrogen bond donor/acceptor functionality, and potential metabolic-site for identifying robust metabolically stable structure.

Subsequently, to achieve high level peripheral and/or spinal cord exposure with peripheral and/or spinal cord selectivity to brain, pharmacokinetic profile of NOP receptor agonist after subcutaneous (sc) administration was investigated, together with its molecular and physicochemical properties, that is, presence manner of hydrophilic functional group, numbers of HBD and HBA, lipophilicity as ACD log $D_{7.4}$ value, and molecular weight (M_W) which would be associated with the general tendency of high plasma levels or low brain penetration in the subcutaneous (systemic) administration condition. Indeed, as representatives, the concentration–time profiles of **1** and **23** in the plasma, spinal cord, cerebrospinal fluid (CSF), and brain after subcutaneous administration in male Sprague–Dawley (SD) rats (10 mg/kg) were measured by HPLC using MS/MS detection. The pharmacokinetics of **1** and **23** are shown in Figure 3.

Thus, compared with the molecular characters of two hydroxymethyl-type analogues, **1** possesses two apparent hydrophilic functionalities at plural sites, that is, one hydroxymethyl group and one secondary-amino group as both HBD and HBA functionalities in the 1- and 2-substituents of the benzimidazole structure, and three tertiary-amino groups as additional HBA functionalities, hence the whole physicochemical properties for **1** were ACD log $D_{7.4}$ = 1.08, M_W = 451.65, HBD = 2, and HBA = 5; and **23** possesses one hydrophilic functionality, that is, one hydroxymethyl group in the 1-portion, and four tertiary-amino groups, hence the whole physicochemical properties for **23** were ACD log $D_{7.4}$ = 3.17, M_W = 439.64, HBD = 1, and HBA = 5. In this pharmacokinetic study, while the systemic circulation was observed for both compounds after subcutaneous administration, the plasma drug levels of **1** appreciably exceeded over those of **23** as expected, which would reflect the difference of the molecular character and metabolic stability in HLM. In detail, the concentrations of **1** at 0.5 and 1.5 h postdose in each tissue were 600 and 504 ng/mL in the plasma, 48 and 63 ng/mL in the spinal cord, 11 and 0 ng/mL in the CSF, and 152 and 226 ng/mL in the brain, respectively (Fig. 3A). By contrast, the concentrations of **23** at 0.5 and 1.5 h postdose in each tissue were 67 and 77 ng/mL in the plasma, 113 and 125 ng/mL in the spinal cord, 5.1 and 7.8 ng/mL in the CSF, and 115 and 197 ng/mL in the brain, respectively (Fig. 3B). Therefore, at 0.5 and 1.5 h postdose, the respective plasma levels of **1** were 8.9- and 6.5-fold greater than those of **23**.

Together, probably because of its far low lipophilicity for the whole structure with more hydrophilic functionalities at plural sites, that is, more number of HBD, the novel designed **1** achieved greater peripherally-selective exposure against brain in the systemic administration compared to **23**.

On the other hand, the NOP receptor agonist whose hydroxymethyl group was converted into non-polar (and/or non-hydrophilic) group such as alkyl group was presumed to have higher blood–brain permeability or higher brain level selectivity in the subcutaneous administration condition relative to the original molecule in the subcutaneous administration condition because of its decreased hydrophilicity under the condition that the other molecular properties of the compound are acceptable to across

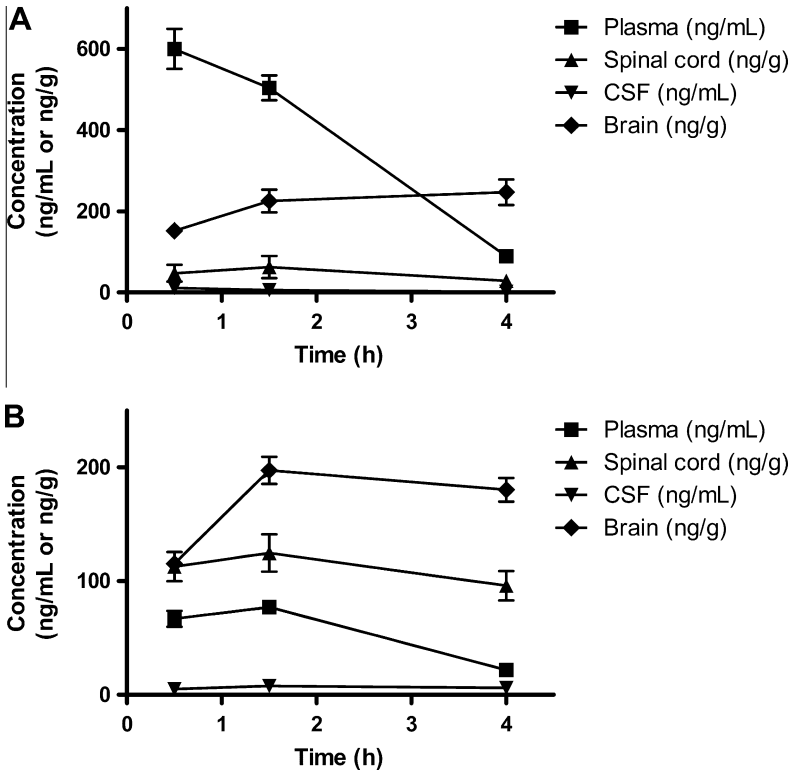

Figure 3. Pharmacokinetic profiles of NOP receptor agonists in rats after subcutaneous administration (10 mg/kg, male SD rats): (A) compound **1**; (B) compound **23**. Data are expressed as means ± SEM of three rats.

BBB. Moreover, the series of methylcyclooctyl-type analogues were investigated expecting brain activity in the oral administration condition with distinctive and appropriate (well-balanced) physicochemical properties as described in detail,[2b,2c] which resulted in the discovery of MCOPPB that showed high oral NOP receptor occupancy in the brain and orally potent anticonflict activity as antianxiety drug. Supplementary, while PCPB, a recently reported brain-active NOP receptor agonist,[24] showed less potency and selectivity for NOP receptor in vitro and weaker oral anxiolytic activity in vivo than those of MCOPPB,[2b,2c] both plasma and brain concentrations of PCPB were similar levels in the oral administration condition (30 mg/kg, 1 h, mice). The difference of the plasma-to-brain exposure ratios between **1** and PCPB in the pharmacokinetic studies would be dependent on both (i) the respective molecular feature, for example, **1** has more number of hydrophilic functionalities with lower lipophilicity for the whole structure relative to PCPB, and (ii) the respective experimental condition such as administration route, that is, subcutaneous (**1**, rats) or oral (PCPB, mice) dosing. For example, compared with the plasma-to-brain ratios (P/B) in the subcutaneous administration condition (10 mg/kg, 0.5 h, male SD rats) for 1,2-substituted benzimidazole analogues, **1** [(hydroxymethyl)cyclooctyl analogue, two HBD functionalities in the 1- and 2-portions of 1,2-substituted benzimidazole structure], **23** [(hydroxymethyl)cyclooctyl analogue, one HBD functionality in the 1-portion], and PCPB (methylcyclooctyl analogue, one HBD functionality in the 2-portion), the rank of orders for the P/B values was P/B = 3.95 for **1** ≫ P/B = 0.58 for **23** > P/B = 0.37 for PCPB.

Overall, it is clear that the molecular properties of **1** such as multisite hydrophilic functionalities and far low lipophilicity for the whole structure with acceptable size and shape contributed to the high and selective plasma exposure in this study. Further pharmacokinetic profile study for the other hydroxymethyl analogues might be also useful to elucidate the factors for plasma selectivity more precisely.

2.3.3. In vivo analgesic effects against mechanical allodynia in the CCI rats

2.3.3.1. Systemic (subcutaneous) administration studies. As the third step, to address the primary endpoint of this study, the analgesic activity of NOP receptor agonist against mechanical allodynia in male SD rats was evaluated by von Frey hair tactile stimulus on chronic constriction injury (CCI) as a clinical relevant model of neuropathic pain via peripheral neuropathy,[4e,4f] of which CCI in the rats was caused by the surgery of loose ligatures around sciatic nerve according to Bennett's method[25] (see Section 4). Especially, the von Frey hair test study in the CCI rats was investigated for the most attractive compound **1** expecting systemic antiallodynic activity with minimized adverse-effects in the subcutaneous administration condition, because of its encouraging characters, that is, highly selective and potent NOP receptor activity in vitro, long-lasting metabolic stability, and high plasma exposure with the high plasma-to-brain ratio in vivo. As well, **27** was investigated for this study to compare with **1**. The results were listed in Table 4.

Actually, systemically (subcutaneously) administered **1** (1.0, 10, and 30 mg/kg) demonstrated long-lasting antiallodynic effects in a dose-dependent manner over the concentration range on the hind-paw ipsilateral to the nerve injury: at 30 min postdose, the minimum effective dose (MED) of the statistically significant activity was 30 mg/kg for 57.6% inhibition ($p < 0.01$ vs CCI/saline group) and the calculated ED_{50} value was 26.8 mg/kg; furthermore at 1.0 h postdose, the antiallodynic effect was increased, that is, the significance was obtained at doses of 10 mg/kg and 30 mg/kg with 37.6% and 79.3% inhibitions, respectively ($p < 0.01$ vs CCI/saline group), and the ED_{50} value was 10.8 mg/kg. Then, the antiallodynic effect was time-dependently reduced: at 2.0 h postdose, the MED was 30 mg/kg with less potent activity (35.8% inhibition, $p < 0.01$ vs CCI/saline group); and at 4.0 h postdose, the effect was not satisfactory significant even at the dose of 30 mg/kg. Meanwhile there was no significant response-change for the sensitivity to the mechanical stimulus on the contralateral uninjured (normal) paw

Table 4
Analgesic effects of NOP receptor agonists against mechanical allodynia in the von Frey hair test on the injured paw of CCI rats after subcutaneous, intrathecal, and intracerebroventricular administrations (male SD rats)

Compound	Treatment			Antiallodynic effect (on the injured paw)		Allodynia-inducing action (on the contralateral normal paw)
	Admin route	Dose	Time	ED_{50}	MED[a]	Response change in the sensitivity
1	sc	1.0, 10, 30 mg/kg	30 min	26.8 mg/kg	30 mg/kg**	No change
			1.0 h	10.8 mg/kg	10 mg/kg**	No change
			2.0 h	>30 mg/kg	30 mg/kg	No change
			4.0 h	>30 mg/kg	NS[a]	No change
1	it	5.5, 55, 170 nmol/site	20 min	80.0 nmol/site	55 nmol/site**	No change
			1.0 h	>170 nmol/site	55 nmol/site*	No change
1	icv	5.5, 55, 170 nmol/site	20 min	>170 nmol/site	55 nmol/site*	No change
			1.0 h	Ineffective	NS	No change
27	sc	1.0, 10, 30 mg/kg	30 min, 1.0 h, 2.0 h, 4.0 h	Ineffective	NS	No change
N/OFQ	it	0.55, 5.5, 55 nmol/site	20 min	10.3 nmol/site	55 nmol/site**	No change
			1.0 h	Ineffective	NS	No change
N/OFQ	icv	0.55, 5.5, 55 nmol/site	20 min	Ineffective	NS	Dose-dependent reduction of the response threshold, 5.5,* 55** nmol/site
			1.0 h	Ineffective	NS	Dose-dependent reduction of the response threshold, 5.5,* 55** nmol/site

** $p < 0.01$ versus CCI/saline group and * $p < 0.05$ versus CCI/saline group for Kruskal-Wallis one way analysis of variance on ranks followed by Tukey test, respectively; significant difference between sham- and CCI-operated groups treated by vehicle was confirmed by *t*-test ($p < 0.01$); $n = 5–6$ for each group.

[a] MED, minimum effective dose in the given dose range; see text for the details of % inhibitions, that is, inhibitory activities against mechanical allodynia in von Frey hair test; NS, not significant.

over the test period for **1** (1.0, 10, and 30 mg/kg, sc; ~4.0 h) compared to pre-administration.

By contrast, **27** showed no significant antiallodynic effect on the injured paw as well as no response-change on the contralateral normal paw in the CCI-operated rats in the test conditions after subcutaneous administration (1.0 mg, 10 mg, and 30 mg/kg; 30 min, 1.0 h, 2.0 h, and 4.0 h).

In this study, the differences for the antiallodynic efficacies between **1** and **27** might be attributable to (i) the difference of the degree of in vitro NOP receptor activity and/or (ii) the difference of molecular properties associated with pharmacokinetic profiles. Concerning the in vitro activity for hNOP receptor, the respective binding affinities and functional activities of these compounds were K_i = 1.438 nM, EC_{50} = 12 nM, E_{max} = 144% for **1**; K_i = 4.54 nM, EC_{50} = 23 nM, E_{max} = 132% for **27**, that is, **1** possesses threefold greater binding affinity and twofold greater functional potency than those of **27**. As for the comparison of physicochemical properties, these compounds have similar molecular sizes (**1**: M_W = 451.65, **27**: M_W = 453.66) and the same numbers of hydrogen bond-related functionalities (HBD = 2 and HBA = 5, respectively), however **1** has lower lipophilicity (ACD log $D_{7.4}$ = 1.08) than **27** (ACD log $D_{7.4}$ = 3.58). Therefore, while **1** showed high plasma exposure levels and the plasma selectivity against brain in vivo, **27** might not have enough plasma exposure levels to show significant in vivo analgesic activity in the subcutaneous administration condition owing to its higher lipophilicity relative to **1**, which was suggested in the pharmacokinetic study for several compounds as mentioned.

Indeed, with the systemic pharmacokinetics in rats for **1** as described, the time-course relationship between antiallodynic activity (sc) and plasma concentration (sc) for **1** (see Table 4 and Fig. 3A) proved the pharmacodynamics regarding the mechanisms of action for time- and concentration-dependent antiallodynic effects after systemic administration of **1**. Thus, subcutaneously administered **1** circulated systemically through blood flow with high plasma exposure and high plasma-to-brain ratio, showing significant antiallodynic effects within 2 h postdose. However the antiallodynic effect of **1** disappeared when the plasma exposure of **1** was markedly diminished at 4 h postdose. Consequently, the high level plasma exposure of **1** was required for the systemically potent antiallodynic efficacy of **1**. In addition, it was indicated that **1** had no potential brain effect that contributes or affects to the systemic analgesic activity during the experimental period including at 4 h postdose, although some brain levels were shown (Fig. 3A). These results strongly suggested that **1** had peripheral- and/or spinal cord-selective analgesic activity in this peripheral nerve injury model.

Besides, further pharmacokinetic study of **27** might be useful to confirm factor for the in vivo activity concerning the above viewpoint. As well, the other analogues might have possibility to show analgesic activity, for example, at local (peripheral or spinal) administration, or might be useful for further in vivo SAR study. For example, **23** and **27**, less potent in vitro and higher lipophilic analogues relative to **1**, might show local analgesic activity if the analogues are given at over certain doses so as to get sufficient peripheral or spinal cord drug levels. However those analogues were not selected for further CCI model study this time, because (i) relative to **1**, those compounds showed less potent in vitro activity or lower metabolic stability, or were thought to be less peripheral exposure and/or selectivity estimated by physicochemical properties or by related pharmacokinetic study, and (ii) the CCI-induced neuropathic pain model study for one compound evaluation needed over several weeks in our conditions including long setting-time, for example, the compound evaluation was performed two weeks after CCI surgery, using not so little number of animals (see Section 4).

2.3.3.2. Local (intrathecal and intracerebroventricular) administration studies. In fact, to get further insight for the mechanisms of the systemic antiallodynic activity of **1** in terms of the site of analgesic action mentioned above, local administration study for **1** in the CCI-induced neuropathic pain rats was performed, which was compared with that of N/OFQ.[26a] These results were also listed in Table 4.

First, after intrathecal (it) administration (5.5, 55, and 170 nmol/site), **1** exhibited significant antiallodynic effects in a dose-dependent manner on the injured paw in the CCI rats, that is, at 20 min postdose, the significance was obtained at 55 and

170 nmol/site with 49.4% and 59.3% inhibitions ($p < 0.01$ vs CCI/saline group), respectively, and the ED_{50} value was 80 nmol/site; and the effect was also shown at 1.0 h postdose in a dose-dependent manner with reduced efficacies, that is, the significance was obtained at 55 and 170 nmol/site with 31.1% and 45.5% inhibitions ($p < 0.05$ and $p < 0.01$ vs CCI/saline group), respectively, that is, the ED_{50} value was greater than 170 nmol/site.

In contrast, after intracerebroventricular (icv) administration (5.5, 55, and 170 nmol/site), **1** showed weak or ineffective antiallodynic effect on the injured paw with no dose related-manner, that is, at 20 min postdose, the MED was 55 nmol/site (23.7% inhibition, $p < 0.05$ vs CCI/saline group) and the ED_{50} value was greater than 170 nmol/site; and the activity was not significant at 1.0 h postdose over the test dosings. In other words, it was clarified that **1** had no or little potential brain effect that contributes to its systemic antiallodynic activity as the primary effect in the CCI model rats, which was also supported by the pharmacokinetics–pharmacodynamics (PK–PD) relationship for **1** as mentioned.

Significantly, the spinal antiallodynic effect of **1** (55 nmol/site; 20 min and 1.0 h) in the CCI rats was blocked by intrathecally administered J-113397, a non-peptide selective NOP receptor antagonist,[22] in a dose-dependent manner (0.55, 5.5, and 55 nmol/site; 20 min and 1.0 h), and completely blocked at 55 nmol/site (20 min and 1.0 h); while J-113397 showed no significant analgesic effect against mechanical allodynia in the CCI rats after subcutaneous dosing (1, 10, and 30 mg/kg, 0.5, 1.0, and 2.0 h). As reported,[26a] [$Nphe^1$]N/OFQ(1–13)NH_2, a peptide NOP receptor antagonist,[7a] showed no significant analgesic effect against mechanical allodynia in the CCI rats after intrathecal or intracerebroventricular dosing (5.5 and 55 nmol/site, 20 min and 1.0 h), as well.

While both systemic and spinal analgesic activities for **1** were indicated in the present systemic and local administration studies, the comparison of the antiallodynic efficacies between administration routes was important. Thus, the subcutaneous administration was significantly effective at 30 min, 1.0 h, and 2.0 h postdose after administration of **1**, for example, the ED_{50} value was 10.8 mg/kg at 1.0 h postdose, and the intrathecal administration was significantly effective at 20 min and 1.0 h postdose, for example, the ED_{50} value was 80.0 nmol/site at 20 min postdose. Hence, regarding to clinical applications for neuropathic pain induced by peripheral neuropathy, the potential of **1** for both systemic (subcutaneous) and intrathecal administrations might be suggested, although further drug-delivery studies would be significant for considering the versatile clinical potential as well. Furthermore, these studies indicated strong possibility of direct analgesic mechanisms driven by the binding of **1** to NOP receptor at peripheral and/or spinal sites, for example, in the peripheral and spinal neurons or DRG, which contribute to the systemic analgesic activity in the subcutaneous administration condition. The peripherally and/or spinally acting analgesic mechanisms were also in line with the described PK–PD relationship for **1**, while the differential effective dose-levels with respective effective periods between systemic and intrathecal administrations were indicated in the studies, and there might be additional possibility associated with the route-differential efficacies for **1** such as administration route-derived distinctive absorption–distribution–metabolism–excretion (ADME) mechanisms or other.

Second, compared to the above results for the non-peptide synthetic agonist **1**, N/OFQ showed similar analgesic effect in the spinal cord whereas complex effects in the brain in our study.[26a] Thus, intrathecally administered N/OFQ (0.55, 5.5, and 55 nmol/site) displayed short-period antiallodynic effects in a dose-dependent manner on the injured paw, that is, at 20 min postdose, the MED was 55 nmol/site ($p < 0.01$ vs CCI/saline group) and the ED_{50} value 10.3 nmol/site; and no antiallodynic effect at 1.0 h postdose. However intracerebroventricularly administrated N/OFQ was ineffective over the test dosings (0.55, 5.5, and 55 nmol/site; 20 min and 1.0 h). Supplementary, independent study with CCI model rats was reported that intrathecally administered morphine showed significant analgesic efficacy against mechanical allodynia at 20 nmol/site as the highest dose in the study, and its analgesic efficacy at 5 min was almost the same as that of intrathecally administered N/OFQ at the same dosage condition (20 nmol/site, 5 min).[26b,26c]

Also, **1** was partially different from N/OFQ for its site-differential actions in other points. Thus, (i) after intracerebroventricular administration, **1** showed weak or no significant antiallodynic effect whereas N/OFQ was completely ineffective or not significant as described. And (ii) intrathecally and intracerebroventricularly administered **1** (5.5, 55, and 170 nmol/site), intrathecally administered N/OFQ (0.55, 5.5, and 55 nmol/site), as well as intracerebroventricularly administered N/OFQ at 0.55 nmol/site showed no response-change on the contralateral normal paw in the CCI rats in the test period from 20 min to 1.0 h postdose, similar to the case of subcutaneously administered **1**; but intracerebroventricularly administered N/OFQ at higher doses showed lower response threshold in a dose-dependent manner to von Frey hair stimuli on the normal paw relative to vehicle, that is, the significance was observed at 5.5 and 55 nmol/site ($p < 0.05$ and < 0.01 vs CCI/saline group, respectively) at 20 min and 1.0 h postdose, which indicated allodynia-inducing action by N/OFQ in this condition.

In conclusion, (i) **1** demonstrated systemically potent antiallodynic activity in the CCI rats based on high plasma exposure and peripherally and/or spinally selective antiallodynic efficacy, and (ii) **1** and N/OFQ showed partially different site-dependent activities in terms of antiallodynic effect and allodynia-inducing action in the local administration study, which would be involved in the differential mechanisms of the actions as discussion later.

2.4. Further safe and selectivity profiles of 1

For the viewpoint of clinical use, high binding- and functional-selectivity for hNOP receptor against human classical opioid peptide receptors was significant for NOP receptor agonist to prevent potential risks for classical opioid peptide receptor-related CNS adverse-effects such as respiratory depression and sedation which are major serious concerns for the treatment of clinical opioid-drugs.[2c] Indeed, highly NOP receptor-selective agonist **1** (as well as **23** or **27**) did not show respiratory depression or sedation effect as observation through the above in vivo experiments at any doses, specifically, in the subcutaneous (up to 30 mg/kg), intrathecal or intracerebroventricular (up to 170 nmol/site) administration conditions for **1**.

Besides, the assessment of the binding affinity of (pre)clinical-drug candidate to human ether-a-go-go related gene (hERG) potassium ion channel is very important for averting potential risk for QT interval prolongation issue in the human heart. Thus, the QT prolongation may relate to abnormal cardiac repolarisation that may lead to Torsades de Pointes in the human heart or sudden death at worst, and the issue is caused by the inhibition of rectifier potassium current (I_{Kr}) in pharmacomedication, of which the potassium ion channels are encoded by hERG in the heart. Indeed, in the evaluation study for the inhibitory activity against [^{3}H]dofetilide binding to hERG potassium ion channel expressed in HEK-293 cells,[2c,27] **1** displayed little hERG ion channel binding affinity, that is, the K_i value was 3700 nM, and the binding selectivity of **1** to hNOP receptor over hERG ion channel was 2573-fold. Therefore, it was estimated that **1** had little potential risk for QT prolongation issue.

Additionally, **1** displayed no significant affinities or effects against 60 off-targets in the screen panel assays in Cerep (Celle l'Evescault, France),[28] thus **1** was inactive for various types of

receptors, transporters, and enzymes that include the targets for neurotransmission mediators, GPCR-related signal transmitters, or specifically, the targets for pain-sensation or -transmission or for inflammation,[3b,4b,4e] such as α_1-, α_2-, β_1-, and β_2-adrenoceptors; muscarinic, γ-aminobutyric acid (GABA), α-amino-3-hydroxy-5-methyl-4-isoxazolepropionate (AMPA), *N*-methyl-D-aspartate (NMDA), benzodiazepine, histamine, dopamine (DA), serotonin (5-HT), and tachykinin receptors; DA, 5-HT, GABA, norepinephrine, and chlorine transporters; and Ca^{2+}, Na^+, and Cl^- channels (see Supplementary data, Table S1). Hence, it is also significant that the structure around **1** is promising for developing highly selective and potent hNOP receptor agonist in further study.

Taken together, all findings of the present studies showed that **1** might establish per se as a potential new-class antiallodynic drug for neuropathic pain induced by peripheral neuropathy, with its potent and dose-dependent systemic analgesic activity in the CCI rats via highly potent and selective (or specific) NOP receptor agonist activity in vitro, and lacks of potential adverse-effects related to classical opioid peptide receptors or hERG potassium ion channel; although further safety-assessment studies including primate model study are indispensible for the establishment of therapeutic indexes toward clinical use.

2.5. Discussion of biological activities including site-differential mechanisms for 1 and N/OFQ

On the other hand, it is significant to compare the antinociceptive effect of **1**, as metabolically stable non-peptide NOP receptor agonist, with that of N/OFQ, as metabolically unstable endogenous peptide ligand.

Thus, in the present study, the systemically potent long-lasting antiallodynic activity of **1** in the CCI neuropathic pain model rats based on the peripheral and/or spinal effect was consistent with the short-period spinal effect of N/OFQ, and the spinal antiallodynic effect of **1** was fully blocked by a NOP receptor antagonist, while it was reported that the [^{35}S]GTPγS binding response stimulated by N/OFQ–NOP receptor binding in the spinal cord was not affected by classical opioid peptide receptor (MOP, KOP or DOP receptor) antagonists or other various GPCR antagonists such as muscarinic, DA, and $GABA_B$ receptor antagonists as well as α_2- and β-adrenoceptor antagonists.[29] Besides N/OFQ has shown (i) analgesic effects for thermal hyperalgesia in CCI rats[9a] and for other peripheral nerve or spinal cord injury-induced neuropathic pain models in rodents,[9b–f] by intrathecal administrations, respectively, and (ii) analgesic effects for acute and peripheral pain- or inflammation models in primates by local peripheral administration (tail)[8f] or by intrathecal administration,[8g] as well as in rodents by intrathecal or peripheral administration.[8a–e]

For a viewpoint of pain-signal processing, NOP receptor activation by N/OFQ shows various, conjugated or integrated blocking effects on pain-sensations or on evoked pain-signal transmissions in the peripheral/spinal cord as mentioned. Besides, it has been reported that NOP receptor mRNA was overexpressed in the ventral horn of lumbar spinal cord on the ipsilateral and contralateral sides of the sciatic nerve injury in CCI rats,[30] and NOP receptor mRNA splice variants were increased in both the ipsilateral lumbar spinal cord and the ipsilateral L5–L6 DRG in CCI rats.[26b] Also it has been reported that (i) the induction of immunoreactivities of both N/OFQ and NOP receptor in the DRG,[31a] and the up-regulations of N/OFQ–NOP receptor binding in the lumber spinal cord[31b] were displayed in neuropathic pain or peripheral inflammation model rats, and (ii) the induction of prepro-N/OFQ mRNA expression in the DRG was displayed in peripheral inflammation model rats.[7g] Hence, these up-regulation phenomena regarding the levels, binding, and immunoreactivities of N/OFQ and NOP receptors in neuropathic pain and/or inflammation states, together with the suppression effects by N/OFQ–NOP receptor system on the evoked pain-signal transmission pathways, would be associated with the origin or enhancement of the peripheral or spinal analgesic action as well as anti-inflammatory action via N/OFQ–NOP receptor system in vivo, while NOP receptor mRNA in the brain was also increased after CCI operation in the rats.[31c]

As well, it is significant that metabolically stable **1** displayed partially different site-dependent antiallodynic efficacies compared to N/OFQ in our disease model study, while pronociceptive or nociceptive responses of major metabolites of N/OFQ in the spinal cord and peripheral[32a,32b] and antinociceptive responses of other metabolites of N/OFQ in the peripheral[8b] have been reported.

Taken collectively, it was clarified that the mechanisms of action for the long-lasting systemic antiallodynic effects of **1** in a dose-dependent manner in the CCI-induced neuropathic pain model rats were derived from its potent and specific NOP receptor agonist activity in response to its potent binding to the receptor in the peripheral and/or spinal cord with its robust metabolic stability in the present study. In other words, **1** established the proof of concept for an intrinsic role of NOP receptor activation in the peripheral and/or spinal cord against neuropathic pain via peripheral neuropathy in vivo. Further analgesic model studies including various types of neuropathic pain models or other disease models are important for exploring and confirming further potential of **1** as analgesic as well as other therapeutic utilities.

Furthermore, the site-dependent discrepancies between **1** and N/OFQ in terms of antiallodynic efficacy and allodynia-inducing action are significant to consider the differential mechanisms underlying them. With this regards, it is noteworthy that the inconsistent actions between N/OFQ and MCOPPB for several in vivo endpoints have been found in our study as reported.[1,2c,2d] Also as an independent study, Ro 64-6198 showed local peripheral (intraperitoneal) or spinal analgesic activity against mechanical or thermal allodynia in rodents, which was limited within the local effects, that is, the compound showed no systemic (subcutaneous) analgesic effect for neuropathic pain,[33a] while robust evidences of different ability to recognize NOP receptor for N/OFQ and Ro 64-6198 have been reported, that is, functional heterogeneity for neurons in the brain tissue,[33b] and different pharmacological profiles in other tissues of different species.[33c]

Besides, functional heterogeneity of NOP receptor depended on the treatment condition of N/OFQ in the mice brain,[34a] functional difference between splice variants of NOP receptor,[34b] and heterogeneity of N/OFQ metabolism that produces different-bioactivity displaying-metabolites in different tissues of different species[34c] have been known. As well, the profile patterns of N/OFQ as well as some ligands in the in vitro functional or binding properties for heterodimers of NOP–KOP-receptors or NOP–MOP-receptors expressed in cultured cells were different from those for NOP receptor monomer,[35a,35b] while as opioid peptide receptor ligands that had spinal cord-specific activity in vivo, an antagonist for the antagonist activity[35c] and an agonist for the analgesic action[35d] associated with site-differential distribution (or organization) for heterodimer of KOP–DOP receptors in vivo have been reported.

Perhaps, some of the above discrepancy or heterogeneity, as well as the metabolic-stability difference between the ligands, might be involved in the partial discrepancy for the site-differential actions between artificial non-peptide agonist **1** and endogenous peptide N/OFQ in terms of differential duration or intensities for the actions and differential signal pathways depended on the sites.

Altogether, **1** revealed its own unique mechanisms, that is, the systemic antinociceptive activity of **1** in the peripheral neuropathy-induced neuropathic pain model rats was driven by the intrinsic agonist activity of peripheral and/or spinal cord NOP receptor, although N/OFQ shows complex activities in several animal models

with various reasons. The discovery of **1** and the present findings including the site-differential activities that were partially inconsistent with those of N/OFQ might be useful for elucidating further underlying mechanisms as well as for variously reported effects (including analgesic effects) via NOP receptor–NOP receptor agonist interaction, and helpful for studying further physiological, pharmacological or neurochemical mechanisms via the NOP receptor–NOP receptor agonist system.

3. Conclusions

In the present strategy, drug design, synthesis, and SAR for 1,2-disubstituted benzimidazole derivatives were investigated to identify peripheral- and/or spinal cord-directed, potent and selective hNOP receptor agonist as systemically potent analgesic for the treatment of neuropathic pain. Indeed, hydrophilic 1-(hydroxymethyl)cyclooctyl group in the 1-substituent was discovered as an indispensable moiety for highly potent, efficacious, and selective NOP receptor activity and high plasma exposure, together with hydrophilic 2-substituent. As the most significant findings, (i) rationally designed **1** {1-[4-(2-{hexahydropyrrolo[3,4-*c*]pyrrol-2(1*H*)-yl}-1*H*-benzimidazol-1-yl)piperidin-1-yl]cyclooctyl}methanol (HPCOM) was identified as the novel non-peptide NOP receptor full agonist that showed potent binding and functional hNOP receptor activities with high selectivity against human classical opioid peptide receptors in vitro, long-lasting metabolic stability, high plasma concentration with high plasma-to-brain selectivity (sc), and systemically potent and dose-dependent antiallodynic activity on injured paw in CCI-induced neuropathic pain model rats (ED_{50} = 10.8 mg/kg, 1 h, sc) derived from peripheral and/or spinal cord-selective antiallodynic activity; (ii) **1** showed no allodynia-inducing action on the contralateral normal paw in the CCI rats, no serious CNS side-effects related to classical opioid peptide receptors such as respiratory depression or sedation as observation up to 30 mg/kg (sc) or 170 nmol/site (it or icv) in this in vivo study, and little hERG potassium ion channel binding. Significantly, these studies including PK–PD relationship and local administration studies for **1** revealed its unique and potentially safe analgesic profiles and mechanisms, which were distinctive from those of N/OFQ in terms of site-differential analgesic efficacy and potential adverse-effect. Consequently, **1** established the proof of concept for peripheral- and/or spinal cord-selective NOP receptor agonist to the systemic antiallodynic activity against neuropathic pain via peripheral neuropathy in vivo. Furthermore, these findings suggest that **1** per se may establish as a potential novel-class analgesic for the treatment of neuropathic pain with the unique mechanisms, although it would be needed to clarify the therapeutic indexes in rats and primates with various analgesic models for **1** as well as further NOP receptor agonist toward clinical-drug candidate. Also, the discovery of **1** and the present findings might be helpful for elucidating further underlying mechanisms of the antinociceptive activity, as well as various physiological, pharmacological or neurochemical mechanisms, associated with the NOP receptor–NOP receptor agonist system.

4. Experimental

4.1. Synthesis

4.1.1. General

In general, reagents, solvents, reagents, and other chemicals were used as purchased without further purification unless noted otherwise. All reactions with air- or moisture-sensitive reactants and solvents were carried out under nitrogen atmosphere unless noted otherwise. Flash column chromatography (medium pressure liquid chromatography) purifications were carried out using Merck silica gel 60 (230–400 mesh ASTM). Preparative thin-layer chromatography (PTLC) purifications were carried out on Merck silica gel 60 F_{254} precoated glass plates at a thickness of 0.5 or 1.0 mm. The structures of all isolated compounds were ensured by NMR, IR, MS or elementary analysis. Nuclear magnetic resonance (^{1}H and ^{13}C NMR) data were determined at 270 MHz on a JNM-LA 270 (JEOL) spectrometer, at 300 MHz on a JNM-LA300 (JEOL) spectrometer, or at 150 or 600 MHz on an AVANCE (Bruker) spectrometer. Chemical shifts are expressed in δ (ppm). ^{1}H NMR chemical shifts were determined relative to tetramethylsilane (TMS) as internal standard. ^{13}C NMR chemical shifts were determined relative to internal TMS at δ 0.0 or to the ^{13}C signal of solvent: $CDCl_3$ δ 77.04, CD_3OD δ 49.8 or DMSO-d_6 δ 39.5. NMR data are reported as follows: chemical shift, number of atoms, multiplicities (s, singlet; d, doublet; t, triplet; q, quartet; m, multiplet; and br, broadened), and coupling constants. ^{1}H–^{1}H correlation spectroscopy (COSY), distortionless enhancement by polarization transfer (DEPT), heteronuclear multiple quantum coherence (HMQC), heteronuclear multiple bond connectivity (HMBC), nuclear Overhauser and exchange spectroscopy (NOESY), and rotating frame nuclear Overhauser and exchange spectroscopy (ROESY) were measured for the determination of ^{1}H–^{1}H and ^{1}H–^{13}C correlations, and the multiplicities by the proton interaction were expressed in ^{13}C NMR data. Infrared spectra were measured by an IR-470 (Shimadzu) infrared spectrometer. Low-resolution mass spectral data (EI) were obtained on an Automass 120 (JEOL) mass spectrometer. Low-resolution mass spectral data (ESI) were obtained on a Quattro II (Micromass) mass spectrometer Agilent 1100 HPLC system. High-resolution mass spectral data (HRMS-FAB) were obtained on a JMS-700 MStation (JEOL) mass spectrometer. Melting point was obtained using Exstar 6000 (Seiko Instruments Inc.) and was uncorrected. The hydrochlorides of **1**, **21**–**23**, **27**, **31**, **33**, **35**, **45**, and **47**, and the salt free **46** were used for pharmacological and/or pharmacokinetic evaluations, respectively.

4.1.2. Synthesis of 1 via 21

4.1.2.1. Methyl 1-aminocyclooctanecarboxylate (11). To a solution of cyclooctanone (31.55 g, 250 mmol) in EtOH (200 mL) and H_2O (180 mL) were added KCN (24.58 g, 378 mmol) and ammonium carbonate (93.69 g, 975 mmol) under N_2. The reaction mixture was stirred at 60 °C under N_2 for 11 h, then concentrated to one-half of the volume, cooled to 0 °C, acidified by adding concentrated HCl, and allowed to stand in the refrigerator at 0 °C for 15 h. The resulting solid was filtered and rinsed with cold H_2O to afford 48.62 g of 1,3-diazaspiro[4.7]dodecane-2,4-dione **9** in 99% yield as a colorless solid. ^{1}H NMR (300 MHz, $CDCl_3$) δ 7.57 (1H, br s), 5.84 (1H, br s), 2.11–1.54 (14H, m). MS (EI direct) *m*/*z*: M^+ 196.

After **9** (48.62 g, 248 mmol) was suspended in 3 N NaOH (611 mL, 1.83 mol) under N_2, the resulting mixture was stirred under reflux conditions under N_2 for 4 days, then cooled to 0 °C. The reaction mixture was adjusted to pH 6 by adding concentrated HCl at 0 °C. The resulting precipitate was filtered, washed with cold H_2O, and then vacuumed at 70 °C for 3 days to give 67.4 g of 1-aminocyclooctanecarboxylic acid **10** (crude) as a white powder. TLC R_f = 0.5 (silica gel, butanol/AcOH/H_2O = 3:1:1, ninhydrin detection).

After **10** (67.4 g) was dissolved in dry MeOH (1.00 L) at room temperature under N_2, the resulting solution was cooled to 0 °C. Dry HCl gas was bubbled into the solution at 0 °C until there was no further increase in weight for the resulting mixture. Then the HCl gas-saturated reaction-mixture was stirred under reflux conditions for 7 h, cooled to room temperature, and concentrated in vacuo. The residue was partitioned between saturated aqueous $NaHCO_3$ (600 mL) and Et_2O (500 mL) at 0 °C. After the organic layer was separated, the aqueous layer was extracted with Et_2O (3× 500 mL). The organic layers were combined, dried over anhydrous

$MgSO_4$, filtered, and concentrated in vacuo to give 31.76 g of the title product **11** in 69% yield from **9** as a slight yellow oil. ^{1}H NMR (300 MHz, $CDCl_3$) δ 3.71 (3H, s), 2.01–1.94 (2H, m), 1.72–1.48 (14H, m). IR (KBr) 1710 cm^{-1} (CO_2Me).

4.1.2.2. 1-Ethyl-1-methyl-4-oxopiperidinium iodide (12). EtI (78.0 mL, 0.975 mol) was slowly added to a solution of 1-methyl-4-piperidone (100 mL, 0.813 mol) in acetone (0.80 L) maintaining at 20–30 °C under N_2. The reaction solution was stirred at the same temperature under N_2 for 17 h. The resulting solid was filtered and washed with acetone, and vacuumed at 90 °C for 4 h to give 170.0 g of the title product **12** in 78% yield as a yellowish-white solid. ^{1}H NMR (300 MHz, $CDCl_3$) δ 3.72 (4H, t, J = 6.57 Hz), 3.58 (2H, q, J = 7.32 Hz), 3.19 (3H, s), 2.81–2.60 (4H, m), 1.32 (3H, t, J = 7.32 Hz).

4.1.2.3. Methyl 1-(4-oxopiperidin-1-yl)cyclooctanecarboxylate (13). A solution of **12** (69.20 g, 257 mmol) in H_2O (128 mL) was gradually added to a refluxing mixture of **11** (31.76 g, 171 mmol) and anhydrous K_2CO_3 (2.37 g, 17.1 mmol) in MeOH (295 mL) under N_2 over a period of 45 min. The reaction mixture was heated to reflux under N_2 for an additional 60 min. More solution of 1-ethyl-1-methyl-4-oxopiperidinium iodide **12** (23.06 g, 85.7 mmol) in H_2O (43.0 mL) was added to the above refluxing mixture over 15 min. The mixture was stirred under reflux conditions for 60 min, then slowly cooled to room temperature with being stirred for 2 h, and then concentrated on a rotary evaporator. The resulting solution was diluted with H_2O (150 mL), then the mixture was extracted with CH_2Cl_2 (2× 150 mL). The organic layers were combined, washed with brine (100 mL) and H_2O (2× 150 mL), dried over anhydrous $MgSO_4$, filtered, and concentrated in vacuo. The residue was purified by flash column chromatography (silica gel, hexane/AcOEt = 4:1) to give 20.24 g of the title product **13** in 44% yield from **11** as a colorless crystalline. ^{1}H NMR (300 MHz, $CDCl_3$) δ 3.67 (3H, s), 2.90 (4H, t, J = 6.03 Hz), 2.40 (4H, t, J = 6.03 Hz), 2.07–1.44 (14H, m).

4.1.2.4. Methyl 1-[4-(hydroxyimino)piperidin-1-yl]cyclooctanecarboxylate (14). To a solution of **13** (9.625 g, 36.0 mmol) in dry MeOH (200 mL) was added a solution of $NH_2OH{\cdot}HCl$ (3.752 g, 54.0 mmol) and AcONa (4.43 g, 54.0 mmol) in dry MeOH (200 mL) at room temperature under N_2. The reaction solution was stirred at room temperature under N_2 for 18 h, then concentrated in vacuo. The residue was cooled to 0 °C, basified by adding saturated aqueous $NaHCO_3$ (150 mL) at the same low temperature, then the mixture was extracted with CH_2Cl_2 (4× 100 mL). The organic layers were combined, dried over anhydrous $MgSO_4$, filtered, and concentrated in vacuo to give 10.74 g of the title product **14** as a slight yellow oil (crude). ^{1}H NMR (270 MHz, $CDCl_3$) δ 7.23 (1H, br s), 3.65 (3H, s), 2.74–2.65 (4H, m), 2.60–2.55 (2H, m), 2.29 (2H, t, J = 5.62 Hz), 2.02–1.89 (4H, m), 1.84–1.32 (10H, m).

4.1.2.5. Methyl 1-(4-aminopiperidin-1-yl)cyclooctanecarboxylate (15). To a solution of **14** (10.72 g, crude) in 10% HCl/MeOH (240 mL) was added PtO_2 (1.6 g). The mixture was stirred at room temperature under H_2 at 1 atm for 36 h then filtered. The filtrate was concentrated in vacuo, and the residue was cooled to 0 °C, basified by adding saturated aqueous $NaHCO_3$ at the same low temperature, then the mixture was extracted with CH_2Cl_2 (3× 200 mL). The organic layers were combined, dried over anhydrous $MgSO_4$, filtered, and concentrated in vacuo to give 8.35 g of the title product **15** in 86% yield from **13** (two steps) as a colorless oil. ^{1}H NMR (300 MHz, $CDCl_3$) δ 3.66 (3H, s), 2.95 (2H, d, J = 12.1 Hz), 2.66–2.56 (1H, m), 2.13 (2H, t, J = 11.7 Hz), 1.94–1.21 (20H, m).

4.1.2.6. Methyl 1-{4-[(2-nitrophenyl)amino]piperidin-1-yl}cyclooctanecarboxylate (16). To a solution of **15** (8.35 g, 31.1 mmol) in dry CH_3CN (295 mL) was added anhydrous K_2CO_3 (6.17 g, 44.6 mmol) followed by 1-fluoro-2-nitrobenzene (3.61 mL, 34.2 mmol) under N_2. The reaction mixture was stirred under reflux conditions under N_2 for 13 h, then, cooled to room temperature and concentrated in vacuo. The residue was partitioned between CH_2Cl_2 (300 mL) and H_2O (250 mL). The organic layer was separated, and the aqueous layer was extracted with CH_2Cl_2 (3× 250 mL). The organic layers were combined, washed with H_2O (250 mL), dried over anhydrous $MgSO_4$, filtered, and concentrated in vacuo. The residue was purified by flash column chromatography (silica gel, hexane/AcOEt = 12:1 to 10:1) to give 5.41 g of the title product **16** in 45% yield as yellow solid. This yield was not an optimized result, compared with the good conversion in the reaction. ^{1}H NMR (300 MHz, $CDCl_3$) δ 8.17 (1H, d, J = 8.61 Hz), 8.11 (1H, br d, J = 7.14 Hz), 7.40 (1H, dd, J = 7.89, 7.68 Hz), 6.85 (1H, d, J = 8.61 Hz), 6.61 (1H, dd, J = 8.61, 7.14 Hz), 3.70 (3H, s), 3.60–3.45 (1H, m), 3.00 (2H, d, J = 12.27 Hz), 2.38 (2H, t, J = 11.88 Hz), 2.10–1.35 (18H, m).

4.1.2.7. Methyl 1-{4-[(2-aminophenyl)amino]piperidin-1-yl}cyclooctanecarboxylate (17). A mixture of **16** (5.41 g, 13.9 mmol), Zn powder (9.08 g, 139 mmol), and NH_4Cl (5.94 g, 111 mmol) in MeOH (46 mL)–THF (92 mL)–H_2O (9.6 mL) was vigorously stirred at room temperature under N_2 for 20 h. The reaction mixture was filtered through a Celite pad with MeOH–THF washing, and then the filtrate was concentrated in vacuo. The residue was partitioned between CH_2Cl_2 (200 mL) and H_2O (200 mL). The organic layer was separated, and the aqueous layer was extracted with CH_2Cl_2 (3× 200 mL). The organic layers were combined, washed with H_2O (250 mL), dried over anhydrous $MgSO_4$, filtered, and concentrated in vacuo to give 4.68 g of the title product **17** in 94% yield as a brown oil. On the other hand, the use of Zn dust instead of the above Zn powder gave insufficient result, that is, complex products for this step. Compound **17**: ^{1}H NMR (300 MHz, $CDCl_3$) δ 6.81–6.65 (4H, m), 3.68 (3H, s), 3.23 (1H, m), 3.00 (2H, d, J = 10.6 Hz), 2.27 (2H, t, J = 11.1 Hz), 2.05–1.35 (21H, m).

4.1.2.8. Methyl 1-[4-(2-oxo-2,3-dihydro-1*H*-benzimidazol-1-yl)-piperidin-1-yl]cyclooctanecarboxylate (18). To a solution of **17** (4.56 g, 12.7 mmol) in anhydrous THF (80.0 mL) was added a solution of 1,1′-carbodiimidazole (CDI) (2.47 g, 15.2 mmol) in THF (60.0 mL) at 0 °C under N_2. The resulting solution was warmed to room temperature and stirred under N_2 for 20 h, and then concentrated in vacuo. The residue was partitioned between CH_2Cl_2 (150 mL) and H_2O (150 mL). The organic layer was separated, and the aqueous layer was extracted with CH_2Cl_2 (4× 150 mL). The organic layers were combined, dried over anhydrous $MgSO_4$, filtered, and concentrated in vacuo. The residue was purified by flash column chromatography (silica gel, CH_2Cl_2/MeOH = 26:1) to afford a brown solid, which was recrystallized from CH_2Cl_2–hexane to give 3.51 g of the title product **18** in 72% yield as a slight brownish-white crystalline. ^{1}H NMR (300 MHz, $CDCl_3$) δ 9.02 (1H, br s), 7.26–7.22 (1H, m), 7.11–7.04 (3H, m), 4.40–4.25 (1H, m), 3.70 (3H, s), 3.20 (2H, d, J = 7.86 Hz), 2.42–2.27 (4H, m), 2.00–1.96 (4H, m), 1.90–1.35 (12H, m).

4.1.2.9. Methyl 1-[4-(2-chloro-1*H*-benzimidazol-1-yl)piperidin-1-yl]cyclooctanecarboxylate (19). A stirring mixture of **18** (964 mg, 2.50 mmol) and $POCl_3$ (30.0 mL, 328 mmol) was warmed using an oil bath (~110 °C) under N_2. After being stirred for 1 h, the resulting solution was warmed up to reflux conditions (the oil bath temperature ~120 °C), stirred under N_2 for 4 h, then cooled to room temperature, and concentrated in vacuo. The residue was cooled to 0 °C, diluted with $CHCl_3$ (30 mL). The cooled solution was poured into H_2O (25 mL) little by little at 0 °C, then the mixture was neutralized by adding 25% aqueous ammonia at 0 °C.

The organic layer was separated, and the aqueous layer was extracted with $CHCl_3$ (4× 30 mL). The organic layers were combined, washed with brine (25 mL), dried over anhydrous $MgSO_4$, filtered, and concentrated in vacuo. The residue was purified by flash column chromatography (silica gel, CH_2Cl_2/MeOH = 70:1) to give 758.3 mg of the title product **19** in 75% yield as a slight brownish-white solid. ^{1}H NMR (300 MHz, $CDCl_3$) δ 7.71–7.67 (2H, m), 7.59–7.56 (2H, m), 4.51–4.40 (1H, m), 3.72 (3H, s), 3.27 (2H, d, J = 10.2 Hz), 2.52–2.31 (4H, m), 2.02–1.98 (4H, m), 1.93–1.40 (12H, m).

4.1.2.10. Methyl 1-[4-(2-{5-benzylhexahydropyrrolo[3,4-*c*]pyrrol-2(1*H*)-yl}-1*H*-benzimidazol-1-yl)piperidin-1-yl]cyclooctanecarboxylate (20). A solution of **19** (563.8 mg, 1.40 mmol) and 2-benzyloctahydropyrrolo[3,4-*c*]pyrrole [^{1}H NMR (300 MHz, $CDCl_3$) δ 7.33–7.25 (5H, m), 3.52 (2H, s), 2.95–2.55 (8H, m), 2.34 (2H, d, J = 6.60 Hz), 1.91 (1H, br s)][18] (664.5 mg, 3.28 mmol) in dry MeOH (6.0 mL) was stirred at 120 °C under N_2 for 86 h in a sealed-tube, cooled to room temperature, then concentrated in vacuo. The residue was partitioned between CH_2Cl_2 (80 mL) and H_2O (80 mL). The organic layer was separated, and the aqueous layer was extracted with $CHCl_3$ (3× 80 mL). The organic layers were combined, dried over anhydrous $MgSO_4$, filtered, and concentrated in vacuo. The residue was purified by flash column chromatography (silica gel, CH_2Cl_2/MeOH = 16:1) to give 403.9 mg of the title product **20** in 51% yield as white solid. ^{1}H NMR (270 MHz, $CDCl_3$) δ 7.61–7.58 (1H, m), 7.47–7.44 (1H, m), 7.36–7.08 (7H, m), 4.28–4.16 (1H, m), 3.70 (3H, s), 3.62 (2H, s), 3.55–3.49 (2H, m), 3.28–3.15 (4H, m), 2.93 (2H, m), 2.72–2.67 (2H, m), 2.51–2.26 (6H, m), 2.03–1.40 (16 H, m). MS (EI direct) m/z: M^+ 569.

4.1.2.11. {1-[4-(2-{5-Benzylhexahydropyrrolo[3,4-*c*]pyrrol-2(1*H*)-yl}-1*H*-benzimidazol-1-yl)piperidin-1-yl]cyclooctyl}methanol (21). To a solution of **20** (403.9 mg, 0.709 mmol) in anhydrous Et_2O (10.0 mL) was added lithium aluminum hydride (LAH) (40.4 mg, 1.06 mmol) at 0 °C under N_2. The reaction mixture was allowed to room temperature, stirred under N_2 for 16 h, cooled to 0 °C, and then AcOEt (5 mL) was added. The mixture was warmed to room temperature, stirred for 20 min, cooled to 0 °C, then H_2O (7 mL) was added dropwise. The mixture was stirred at 0 °C for 10 min, allowed to room temperature, and stirred for 1 h. The organic layer was separated, and the aqueous layer was extracted with AcOEt (4× 15 mL). The organic layers were combined, dried over anhydrous $MgSO_4$, filtered, and concentrated in vacuo. The residue was purified by flash column chromatography (silica gel, CH_2Cl_2/MeOH = 10:1, then CH_2Cl_2/MeOH/25% aqueous ammonia = 100:10:1) to give 369.8 mg of the title product **21** in 96% yield as a white solid. ^{1}H NMR (300 MHz, $CDCl_3$) δ 7.61–7.58 (1H, m), 7.43–7.22 (6H, m), 7.18–7.08 (2H, m), 4.33–4.18 (1H, m), 3.63 (2H, s), 3.55–3.49 (2H, m), 3.39 (2H, s), 3.32–3.16 (4H, m), 2.99–2.89 (2H, m), 2.76–2.65 (2H, m), 2.55–2.40 (6H, m), 1.95–1.40 (17H, m). *HCl salt formation of* **21** *(general procedure):* After **21** (23.8 mg, 0.0434 mmol) was dissolved in dry CH_2Cl_2 (20 mL) and excess equivalent of 10% HCl/MeOH solution (30 mL), the resulting solution was stirred at room temperature, then the solvent was concentrated in vacuo. The residue was collected and vacuumed at 60 °C to give 18.0 mg of the corresponding trihydrochloride as a white solid: ^{13}C NMR (150 MHz, CD_3OD) δ 153.3 (1C, s), 146.8 (1C, s), 133.0/132.5 (2C, d), 132.5 (1C, s), 132.1/131.4 (1C, s), 131.9 (2C, d), 131.2/131.0 (1C, d), 127.0 (1C, d), 126.0 (1C, d), 115.8/115.7 (1C, d), 114.3 (1C, d), 75.8 (1C, s), 63.3/63.1 (1C, t), 61.1/59.6 (1C, t), 59.3/58.9 (2C, t), 56.6/56.4 (2C, t), 54.7/54.5 (1C, d), 48.4/48.2 (2C, t), 43.9/43.4 (2C, d), 30.1 (2C, t), 29.1 (2C, t), 28.8 (2C, t), 27.7 (1C, t), 25.5/25.4 (2C, t). IR (KBr): 3368, 2932, 1647, 1541, 1458, 1059, 758 cm^{-1}. Anal. Calcd for $C_{34}H_{47}N_5O{\cdot}3HCl{\cdot}3H_2O$: C, 57.91; H, 8.00; N, 9.93. Found: C, 57.76; H, 8.10; N, 9.82.

4.1.2.12. {1-[4-(2-{Hexahydropyrrolo[3,4-*c*]pyrrol-2(1*H*)-yl}-1*H*-benzimidazol-1-yl)piperidin-1-yl]cyclooctyl}methanol (1), HPCOM. A mixture of **21** (salt free, 361.9 mg, 0.668 mmol) and $Pd(OH)_2$ (70.6 mg) in MeOH (10.0 mL) was stirred at room temperature under H_2 at 1 atm for 2 days. The Pd catalyst was filtered off, and the filtrate was concentrated in vacuo. The residue was purified by flash column chromatography (silica gel, CH_2Cl_2/MeOH = 10:1, then CH_2Cl_2/MeOH/25% aqueous ammonia = 200:20:1) to give 276.1 mg of the title product **1** in 92% yield as a white solid. ^{1}H NMR (300 MHz, $CDCl_3$) δ 7.61–7.58 (1H, m), 7.43–7.40 (1H, m), 7.18–7.09 (2H, m), 4.30–4.15 (1H, m), 3.55–3.50 (2H, m), 3.39 (2H, s), 3.29–3.26 (2H, m), 3.17–3.11 (4H, m), 2.94–2.80 (4H, m), 2.50–2.35 (4H, m), 1.98–1.42 (18H, m). MS (ESI positive) m/z: $[M+H]^+$ 452. According to the general procedure to form HCl salt, **1** (276.1 mg) was converted into 257.0 mg of the corresponding trihydrochloride: HPLC analysis: chemical purity of 99% with no impurity over 0.5% [apparatus: Alliance 2690 with PDA detector, Waters RP03; analytical column, Kromasil 5C4, 250 × 4.6 mm, 5 μm (particle size); eluent, CH_3CN/0.3% $HClO_4$ = 25:75; flow rate, 1.0 mL/min), column temperature, 35 °C; UV detection: 210 nm, retention time, 18 min]. Full assignments of ^{1}H NMR (600 MHz, CD_3OD) and ^{13}C NMR (150 MHz, CD_3OD) data, and key 2D NMR correlations were shown in Table 1 and Figure 2, respectively. IR (KBr) cm^{-1}: 3387, 2934, 1636, 1616, 1479, 1456, 1398, 1379, 1302, 1057, 837, 760. MS (ESI positive) m/z: $[M+H]^+$ 452.30. Anal. Calcd for $C_{27}H_{41}N_5O{\cdot}3HCl{\cdot}0.78H_2O$: C, 56.39; H, 7.99; N, 12.18. Found: C, 56.66; H, 8.22; N, 11.89.

4.1.3. Synthesis of 22, 23, 27, and 31

4.1.3.1. Methyl 1-{4-[2-(4-methylpiperazin-1-yl)-1*H*-benzimidazol-1-yl]piperidin-1-yl}cyclooctanecarboxylate (22). A mixture of **19** (757.0 mg, 1.87 mmol) and 1-methylpiperazine (9.80 mL, 88.4 mmol) was stirred at 110 °C under N_2 for 24 h in a round-bottomed flask equipped with a reflux condenser, cooled to room temperature, then concentrated in vacuo. The residue was partitioned between CH_2Cl_2 (40 mL) and H_2O (30 mL). The organic layer was separated, and the aqueous layer was extracted with $CHCl_3$ (5× 40 mL). The organic layers were combined, dried over anhydrous $MgSO_4$, filtered, and concentrated in vacuo. The residue was purified by flash column chromatography (silica gel, CH_2Cl_2/MeOH = 15:1) to give 671.7 mg of the title product **22** in 77% yield as a white solid. ^{1}H NMR (270 MHz, $CDCl_3$) δ 7.65–7.60 (1H, m), 7.50–7.43 (1H, m), 7.20–7.11 (2H, m), 4.20–4.08 (1H, m), 3.72 (3H, s), 3.30–3.21 (6H, m), 2.65–2.59 (4H, m), 2.52–2.25 (4H, m), 2.38 (3H, s), 2.06–1.93 (4H, m), 1.90–1.38 (12H, m). According to the general procedure to form HCl salt, **22** was converted into the corresponding trihydrochloride: ^{13}C NMR (150 MHz, CD_3OD) δ 171.1 (1C, s), 155.0 (1C, s), 134.0 (1C, s), 131.8 (1C, s), 127.1 (1C, d), 126.8 (1C, d), 116.4 (1C, d), 116.0 (1C, d), 79.4 (1C, s), 55.3 (1C, q), 54.6 (1C, d), 54.4 (2C, t), 50.3 (2C, t), 50.0 (2C, t), 44.6 (1C, q), 29.7 (2C, t), 29.3 (2C, t), 28.6 (2C, t), 27.3 (1C, t), 25.5 (2C, t). IR (KBr): 3422, 2930, 2658, 2684, 1744, 1632, 1612, 1477, 1458, 1265, 1211, 972, 762 cm^{-1}. Anal. Calcd for $C_{27}H_{41}N_5O_2{\cdot}3HCl{\cdot}0.65H_2O{\cdot}0.2MeOH$: C, 54.89; H, 7.81; N, 11.77. Found: C, 55.27; H, 8.20; N, 11.96.

4.1.3.2. (1-{4-[2-(4-Methylpiperazin-1-yl)-1*H*-benzimidazol-1-yl]piperidin-1-yl}cyclooctyl)methanol (23). To a solution of **22** (salt free, 190.1 mg, 0.407 mmol) in anhydrous THF (5.0 mL) was added LAH (23.1 mg, 0.609 mmol) at 0 °C under N_2. The reaction mixture was allowed to room temperature, stirred under N_2 for 10 h, and then cooled to 0 °C. AcOEt (10 mL) was added to the reaction solution at 0 °C, allowed to room temperature, then stirred for 1 h. The mixture was cooled to 0 °C, then H_2O (10 mL) was added dropwise, allowed to room temperature, and stirred at room temperature for 1 h. The organic layer was separated, and the aqueous

layer was extracted with AcOEt (4× 15 mL). The organic layers were combined, dried over anhydrous $MgSO_4$, filtered, and concentrated in vacuo. The residue was purified by flash column chromatography (silica gel, CH_2Cl_2/MeOH = 15:1, then 9:1) to give 154.7 mg of the title product **23** in 87% yield as a white solid. ^{1}H NMR (300 MHz, $CDCl_3$) δ 7.64–7.60 (1H, m), 7.45–7.43 (1H, m), 7.20–7.10 (2H, m), 4.24–4.10 (1H, m), 3.39 (2H, s), 3.29–3.26 (6H, m), 2.68–2.60 (4H, m), 2.50–2.37 (7H, m), 1.98–1.38 (17H, m). MS (EI direct) *m*/*z*: M^+ 439. According to the general procedure to form HCl salt, **23** was converted into the corresponding trihydrochloride: ^{13}C NMR (150 MHz, CD_3OD) δ 154.5 (1C, s), 131.4 (1C, s), 131.4 (1C, s), 127.0 (1C, d), 126.5 (1C, d), 116.0 (1C, d), 115.5 (1C, d), 75.6 (1C, s), 62.9 (1C, t), 54.7 (1C, d), 54.2 (2C, t), 49.7 (2C, t), 48.1 (2C, t), 44.4 (1C, q), 29.8 (2C, t), 28.5 (2C, t), 28.4 (2C, t), 27.4 (1C, t), 25.1 (2C, t). IR (KBr): 3387, 2928, 2694, 1630, 1612, 1475, 1458, 1396, 1269, 1140, 1057, 972, 760 cm^{-1}. Anal. Calcd for $C_{26}H_{41}N_5O{\cdot}3HCl{\cdot}0.4H_2O{\cdot}0.2MeOH$: C, 55.93; H, 8.17; N, 12.45. Found: C, 56.08; H, 8.54; N, 12.54.

4.1.3.3. Methyl 1-{4-[2-(3,3-dimethylpiperazin-1-yl)-1*H*-benzimidazol-1-yl]piperidin-1-yl}cyclooctanecarboxylate (24). To a solution of 2,2-dimethylpiperazine (305.0 mg, 2.67 mmol) in dry MeOH (2.0 mL) was added **19** (338.5 mg, 0.838 mmol) with dry MeOH (2.0 mL) and dry CH_2Cl_2 (1.0 mL). The volume of the resulting solution was reduced to ~0.5 mL by dryer heating, and then dry MeOH (2.0 mL) was added to the solution. The resulting solution was stirred at 120 °C under N_2 for 45 h in a sealed-tube, cooled to room temperature, then concentrated in vacuo. The residue was purified by PTLC (silica gel, CH_2Cl_2/MeOH = 10:1) to give 224.1 mg of the title product **24** in 56% yield as a white solid. ^{1}H NMR (270 MHz, $CDCl_3$) δ 7.65–7.58 (1H, m), 7.52–7.44 (1H, m), 7.21–7.12 (2H, m), 4.28–4.13 (1H, m), 3.72 (3H, s), 3.35–3.05 (9H, m), 2.52–2.37 (2H, m), 2.28 (2H, t, *J* = 12.0 Hz), 2.08–1.92 (4H, m), 1.89–1.38 (18H, m).

4.1.3.4. Methyl 1-{4-[2-(4-benzyl-3,3-dimethylpiperazin-1-yl)-1*H*-benzimidazol-1-yl]piperidin-1-yl}cyclooctanecarboxylate (25). To a mixture of **24** (224.1 mg, 0.465 mmol) and anhydrous K_2CO_3 (96.7 mg, 0.700 mmol) in dry toluene (8.0 mL) was added benzyl bromide (119.7 mg, 0.700 mmol) at room temperature under N_2. The reaction mixture was stirred under reflux conditions under N_2 for 20 h, cooled to room temperature, and then H_2O (25 mL) was added dropwise. The mixture was extracted with CH_2Cl_2 (1× 50 mL, 4× 30 mL). The organic layers were combined, dried over anhydrous $MgSO_4$, filtered, and concentrated in vacuo. The residue was purified by PTLC (silica gel, CH_2Cl_2/MeOH = 10:1) to give 162.0 mg of the title product **25** in 61% yield. ^{1}H NMR (270 MHz, $CDCl_3$) δ 7.65–7.59 (1H, m), 7.50–7.44 (1H, m), 7.42–7.21 (5H, m), 7.29–7.10 (2H, m), 4.40–4.20 (1H, m), 3.72 (3H, s), 3.61 (2H, s), 3.25 (2H, d, *J* = 11.2 Hz), 3.16–3.13 (2H, m), 3.04 (2H, s), 2.65–2.61 (2H, m), 2.45 (2H, dq, *J* = 11.9 Hz), 2.29 (2H, t, *J* = 11.7 Hz), 2.06–1.40 (16H, m), 1.27 (6H, s).

4.1.3.5. (1-{4-[2-(4-Benzyl-3,3-dimethylpiperazin-1-yl)-1*H*-benzimidazol-1-yl]piperidin-1-yl}cyclooctyl)methanol (26). To a solution of **25** (162.0 mg, 0.283 mmol) in anhydrous THF (3.5 mL) was added LAH (21.5 mg, 0.567 mmol) at 0 °C under N_2. The reaction mixture was allowed to room temperature, stirred under N_2 for 21 h, cooled to 0 °C, and then AcOEt (30 mL) was added. The mixture was stirred for 10 min at 0 °C, allowed to room temperature, stirred for 20 min, and then cooled to 0 °C. H_2O (30 mL) was added dropwise to the mixture at 0 °C, and the mixture was stirred for 10 min, allowed to room temperature, and stirred at room temperature for 1 h. The organic layer was separated, and the aqueous layer was extracted with AcOEt (3× 30 mL). The organic layers were combined, dried over anhydrous $MgSO_4$, filtered, and concentrated in vacuo. The residue was purified by PTLC (silica gel, CH_2Cl_2/MeOH = 10:1) to give 141.2 mg of the title product **26** in 92% yield as a brown solid. ^{1}H NMR (300 MHz, $CDCl_3$) δ 7.64–7.61 (1H, m), 7.47–7.21 (6H, m), 7.19–7.10 (2H, m), 4.39–4.22 (1H, m), 3.62 (2H, s), 3.40 (2H, s), 3.32–3.20 (2H, m), 3.18–3.20 (2H, m), 3.05 (2H, s), 2.66–2.62 (2H, m), 2.51–2.35 (4H, m), 1.98–1.50 (17H, m), 1.28 (6H, s).

4.1.3.6. (1-{4-[2-(3,3-Dimethylpiperazin-1-yl)-1*H*-benzimidazol-1-yl]piperidin-1-yl}cyclooctyl)methanol (27). A mixture of **26** (141.2 mg, 0.260 mmol) and $Pd(OH)_2$ (30.0 mg) in MeOH (4.0 mL) was stirred at room temperature under H_2 at 1 atm for 2 days. The Pd catalyst was filtered off, and the filtrate was concentrated in vacuo. The residue was purified by flash column chromatography (silica gel, CH_2Cl_2/MeOH/25% aqueous ammonia = 100:10:1) to give 94.1 mg of the title product **27** in 80% yield as a white solid. ^{1}H NMR (270 MHz, $CDCl_3$) δ 7.66–7.60 (1H, m), 7.48–7.42 (1H, m), 7.21–7.11 (2H, m), 4.37–4.23 (1H, m), 3.40 (2H, s), 3.29 (2H, d, *J* = 6.26 Hz), 3.14 (4H, s), 2.94 (2H, s), 2.52–2.37 (4H, m), 2.04–1.40 (18H, m), 1.30 (6H, s). MS (EI direct) *m*/*z*: M^+ 453. Compound **27** was converted into of the corresponding trihydrochloride: ^{13}C NMR (150 MHz, CD_3OD) δ 155.0 (1C, s), 133.3 (1C, s), 131.6 (1C, s), 127.4 (1C, d), 126.9 (1C, d), 116.2 (1C, d), 116.1 (1C, d), 76.0 (1C, s), 63.4 (1C, t), 58.8 (1C, t), 56.7 (1C, s), 55.0 (1C, d), 50.5 (1C, t), 48.4 (2C, t), 41.1 (1C, t), 30.1 (2C, t), 28.8 (2C, t), 28.7 (2C, t), 27.6 (1C, t), 25.3 (2C, t), 24.0 (2C, q). Anal. Calcd for $C_{27}H_{43}N_5O{\cdot}3HCl{\cdot}1.55H_2O{\cdot}0.6MeOH$: C, 54.33; H, 8.51; N, 11.48. Found: C, 54.71; H, 8.90; N, 11.49.

4.1.3.7. Methyl 1-{4-[2-(3-methylpiperazin-1-yl)-1*H*-benzimidazol-1-yl]piperidin-1-yl}cyclooctanecarboxylate (28). A solution of **19** (90.0 mg, 0.223 mmol) and 2-methylpiperazine (111.7 mg, 1.12 mmol) in dry MeOH (20.0 mL) was stirred at 120 °C under N_2 for 2 days in a sealed-tube, then cooled to room temperature, and concentrated in vacuo. The residue was purified by PTLC (silica gel, CH_2Cl_2/MeOH = 10:1) to give 71.4 mg of the title product **28** in 68% yield as a white solid. ^{1}H NMR (270 MHz, $CDCl_3$) δ 7.65–7.61 (1H, m), 7.50–7.46 (1H, m), 7.18–7.14 (2H, m), 4.25–4.10 (1H, m), 3.72 (3H, s), 3.28–2.95 (9H, m), 2.80–2.72 (1H, m), 2.53–2.25 (4H, m), 2.01–1.40 (16 H, m), 1.13 (3H, d, *J* = 6.43 Hz).

4.1.3.8. Methyl 1-{4-[2-(4-benzyl-3-methylpiperazin-1-yl)-1*H*-benzimidazol-1-yl]piperidin-1-yl}cyclooctanecarboxylate (29). To a mixture of **28** (71.4 mg, 0.153 mmol) and anhydrous K_2CO_3 (31.8 mg, 0.230 mmol) in dry toluene (2.5 mL) was added benzyl bromide (39.3 mg, 0.230 mmol) at room temperature under N_2. The reaction mixture was stirred under reflux conditions under N_2 for 22 h, cooled to room temperature, then H_2O (5 mL) was added dropwise. The mixture was extracted with CH_2Cl_2 (3× 20 mL). The organic layers were combined, dried over anhydrous $MgSO_4$, filtered, and concentrated in vacuo. The residue was purified by PTLC (silica gel, CH_2Cl_2/MeOH = 15:1) to give 45.5 mg of the title product **29** in 53% yield. ^{1}H NMR (270 MHz, $CDCl_3$) δ 7.64–7.61 (1H, m), 7.48–7.10 (8H, m), 4.24–4.05 (2H, m), 3.72 (3H, s), 3.32–3.00 (8H, m), 2.85–2.70 (2H, m), 2.50–2.23 (4H, m), 2.00–1.38 (16H, m), 1.25 (3H, d, *J* = 6.24 Hz).

4.1.3.9. (1-{4-[2-(4-Benzyl-3-methylpiperazin-1-yl)-1*H*-benzimidazol-1-yl]piperidin-1-yl}cyclooctyl)methanol (30). To a solution of **29** (43.9 mg, 0.0787 mmol) in anhydrous THF was added LAH (5.8 mg, 0.15 mmol) at 0 °C under N_2. The reaction mixture was allowed to room temperature, then stirred under N_2 for 2 h. The reaction mixture was cooled to 0 °C, then AcOEt (5 mL) was added, and the mixture was stirred at room temperature for a while, then H_2O (5 mL) was added. The mixture was stirred at room temperature for 5 min, then the mixture was extracted with

AcOEt (3× 20 mL), dried over anhydrous $MgSO_4$, filtered, and concentrated in vacuo to afford 38.8 mg of title product **30** in 93% yield as a pale yellowish-white solid. This compound was used for the next reaction without further purification. ^{1}H NMR (270 MHz, $CDCl_3$) δ 7.64–7.61 (1H, m), 7.44–7.08 (8H, m), 4.25–4.08 (2H, m), 3.39 (2H, s), 3.31–3.01 (8H, m), 2.88–2.73 (2H, m), 2.50–2.34 (5H, m), 1.97–1.42 (16H, m), 1.25 (3H, d, J = 6.26 Hz).

4.1.3.10. (1-{4-[2-(3-Methylpiperazin-1-yl)-1*H*-benzimidazol-1-yl]piperidin-1-yl}cyclooctyl)methanol (31). A mixture of **30** (38.8 mg, 0.0732 mmol) and 10% Pd/C (7.8 mg) in MeOH (1.0 mL)–10% HCl/MeOH (0.5 mL) was stirred at room temperature under H_2 at 1 atm for 2 days. The Pd catalyst was filtered off, and the filtrate was concentrated on a rotary evaporator. The residue was basified by adding saturated aqueous $NaHCO_3$ at 0 °C, then the mixture was extracted with CH_2Cl_2 (3× 15 mL). The organic layers were combined, dried over anhydrous $MgSO_4$, filtered, and concentrated in vacuo. The residue was purified by PTLC (silica gel, AcOEt/2-propanol/25% NH_4OH = 10:2:1, twice developments on one plate) to give 19.9 mg of the title product **31** in 62% yield as a colorless oil. ^{1}H NMR (270 MHz, $CDCl_3$) δ 7.65–7.61 (1H, m), 7.46–7.43 (1H, m), 7.20–7.10 (2H, m), 4.28–4.14 (1H, m), 3.40 (2H, s), 3.30–2.97 (9H, m), 2.76 (1H, dd, J = 11.9, 10.2 Hz), 2.50–2.36 (4H, m), 1.93–1.45 (17H, m), 1.13 (3H, d, J = 6.26 Hz). Compound **31** was converted into the corresponding trihydrochloride: ^{13}C NMR (150 MHz, CD_3OD) δ 155.2 (1C, s), 134.6 (1C, s), 132.0 (1C, s), 126.9 (1C, d), 126.5 (1C, d), 116.7 (1C, d), 115.6 (1C, d), 75.8 (1C, s), 63.3 (1C, t), 55.3 (1C, t), 54.7 (1C, d), 52.8 (1C, d), 49.5 (1C, t), 48.3 (2C, t), 44.8 (1C, t), 30.2 (1C, t), 30.1 (1C, t), 28.8 (2C, t), 28.8 (2C, t), 27.6 (1C, t), 25.3 (2C, t), 16.9 (1C, q). IR (KBr): 3389, 2932, 1612, 1460, 1393, 1304, 1269, 1138, 1057, 1015, 986, 895, 760 cm^{-1}. MS (ESI positive) m/z: $[M+H]^+$ 440.2. Anal. Calcd for $C_{26}H_{41}N_5O{\cdot}3HCl{\cdot}3.5H_2O$: C, 51.02; H, 8.40; N, 11.44. Found: C, 51.22; H, 8.21; N, 11.73.

4.1.4. Synthesis of 33, 35, and 45

4.1.4.1. Methyl 1-{4-[2-(4-chlorophenyl)-1*H*-benzimidazol-1-yl]piperidin-1-yl}cyclooctanecarboxylate (32). A mixture of **17** (89.9 mg, 0.250 mmol) and 4-chlorobenzaldehyde (35.1 mg, 0.250 mmol) in dry EtOH (2.5 mL) was stirred under reflux conditions under N_2 for 1 h, then allowed to room temperature. The reaction mixture was concentrated in vacuo. The residue was dissolved in benzene (2.5 mL), then $Cu(OAc)_2{\cdot}H_2O$ (36.0 mg, 0.180 mmol) was added to the solution. The mixture was vigorously stirred at room temperature for 1 h, then $Cu(OAc)_2{\cdot}H_2O$ (18.9 mg, 0.0947 mmol) was added. The mixture was stirred for 1 h, then $Cu(OAc)_2{\cdot}H_2O$ (20.0 mg, 0.100 mmol) was added. The mixture was stirred for 2 h, heated briefly to boiling, and then cooled to room temperature. To the reaction mixture was added concentrated HCl–EtOH, then the resulting acidic solution was treated with 5% solution of Na_2S [1.5 equiv of $Cu(OAc)_2$], and the precipitated CuS was removed off by filtration. The filtrate was basified with saturated aqueous $NaHCO_3$ at 0 °C then extracted with AcOEt. The combined organic extracts were dried Na_2SO_4, filtered, concentrated in vacuo. The residue was purified by PTLC (silica gel, AcOEt/hexane = 1:4) to give 16.0 mg of the title product **32** in 13% yield with a small amount of impurity. ^{1}H NMR (300 MHz, $CDCl_3$) δ 7.85–7.27 (8H, m), 4.40–4.23 (1H, m), 3.67 (3H, s), 3.22 (2H, d, J = 11.5 Hz), 2.64–2.50 (2H, m), 2.23–1.40 (18H, m).

4.1.4.2. (1-{4-[2-(4-Chlorophenyl)-1*H*-benzimidazol-1-yl]piperidin-1-yl}cyclooctyl)methanol (33). To a solution of **32** (16.0 mg, 0.0333 mmol) in anhydrous THF (0.5 mL) was added LAH (1.9 mg, 0.050 mmol) at 0 °C under N_2. The reaction mixture was allowed to room temperature, stirred under N_2 for 24 h, and cooled to 0 °C. AcOEt (20 mL) was added to the reaction solution at 0 °C, then the mixture allowed to room temperature, stirred for 1 h, cooled to 0 °C, and then H_2O (15 mL) was added dropwise. The mixture was warmed to room temperature, and stirred for 40 min. The organic layer was separated, and the aqueous layer was extracted with AcOEt (3× 20 mL). The organic layers were combined, dried over anhydrous $MgSO_4$, filtered, and concentrated in vacuo. The residue was purified by flash column chromatography (silica gel, CH_2Cl_2/MeOH = 20:1) to give 4.6 mg of the title product **33** in 31% yield as a white foam. ^{1}H NMR (300 M, $CDCl_3$) δ 7.83–7.79 (1H, m), 7.69–7.64 (1H, m), 7.59–7.50 (4H, m), 7.32–7.26 (2H, m), 4.35–4.24 (1H, m), 3.38 (2H, s), 3.24 (2H, d, J = 10.6 Hz), 2.62–2.48 (2H, m), 2.36 (2H, t, J = 11.9 Hz), 1.96–1.43 (17H, m). Compound **33** was converted into the corresponding dihydrochloride: ^{13}C NMR (150 MHz, CD_3OD) δ 153.7 (1C, s), 140.2 (1C, s), 139.2 (1C, s), 134.0 (1C, s), 133.5 (2C, d), 131.7 (2C, d), 127.1 (1C, d), 127.0 (1C, d), 127.0 (1C, s), 119.1 (1C, d), 115.7 (1C, d), 75.8 (1C, s), 63.2 (1C, t), 55.5 (1C, d), 48.3 (2C, t), 30.1 (2C, t), 29.2 (2C, t), 28.7 (2C, t), 27.6 (1C, t), 25.3 (2C, t). MS (ESI positive) m/z: $[M+H]^+$ 452. HRMS-FAB m/z: exact mass calcd for $C_{27}H_{35}N_3OCl[M+H]^+$, 452.2469; found, 452.2453.

4.1.4.3. Methyl 1-{4-[2-(3-chloro-4-fluorophenyl)-1*H*-benzimidazol-1-yl]piperidin-1-yl}cyclooctanecarboxylate (34). To a stirred solution of 3-chloro-4-fluorobenzoic acid (91.6 mg, 0.525 mmol) and **17** (124.6 mg, 0.347 mmol) in anhydrous THF (4.0 mL) was added water soluble carbodiimide, that is, 1-ethyl-3-(3-dimethylaminopropyl)carbodiimide hydrochloride (WSCI) (124.6 mg, 0.650 mmol) at −20 °C under N_2. The reaction mixture was stirred under N_2 for 10 min at that temperature, warmed to 0 °C, stirred for 10 min, allowed to room temperature then stirred for 2 days. The reaction mixture was cooled to 0 °C, poured into saturated aqueous $NaHCO_3$ (15 mL) at 0 °C, then the mixture was extracted with CH_2Cl_2 (4× 15 mL). The combined extracts were dried over anhydrous $MgSO_4$, and concentrated in vacuo. The residue was mixed with $POCl_3$ (25.0 mL) under N_2, and the resulting mixture was warmed using an oil bath (~110 °C), stirred for 1 h, warmed to reflux (the bath temperature ~120 °C) and stirred for 6 h. The reaction solution was allowed to room temperature, concentrated in vacuo, and then coevaporated with $CHCl_3$ (20 mL). The residue was cooled to 0 °C, diluted with $CHCl_3$ (30 mL), then H_2O (20 mL) was added at 0 °C. The mixture was basified by adding 25% aqueous ammonia at 0 °C. The organic layer was separated, and the aqueous layer was extracted with $CHCl_3$ (4× 30 mL). The organic layers were combined, dried over anhydrous $MgSO_4$, and concentrated in vacuo. The residue was purified by flash column chromatography (silica gel, hexane/AcOEt = 4:1) to give 131.0 mg of the title product **34** in 76% yield from **17**. ^{1}H NMR (300 MHz, $CDCl_3$) δ 7.82–7.79 (1H, m), 7.75–7.68 (2H, m), 7.49–7.44 (1H, m), 7.33–7.27 (3H, m), 4.33–4.20 (1H, m), 3.67 (3H, s), 3.23 (2H, d, J = 11.6 Hz), 2.64–2.50 (2H, m), 2.21 (2H, t, J = 11.9 Hz), 2.04–1.40 (16H, m).

4.1.4.4. (1-{4-[2-(3-Chloro-4-fluorophenyl)-1*H*-benzimidazol-1-yl]piperidin-1-yl}cyclooctyl)methanol (35). To a solution of **34** (113.1 mg, 0.227 mmol) in anhydrous Et_2O (3.0 mL)–anhydrous THF (3.0 mL) was added LAH (12.9 mg, 0.340 mmol) at 0 °C under N_2. The reaction mixture was allowed to room temperature, stirred under N_2 for 2 days then cooled to 0 °C. AcOEt (4 mL) was added to the reaction solution at 0 °C, then the mixture was allowed to room temperature, stirred for 1 h, cooled to 0 °C, then H_2O (10 mL) was added dropwise. The mixture was warmed to allow to room temperature, then stirred for 1 h. The organic layer was separated, and the aqueous layer was extracted with CH_2Cl_2 (5× 15 mL). The organic layers were combined, dried over anhydrous $MgSO_4$, filtered, and concentrated in vacuo. The residue was purified by flash column chromatography (silica gel, CH_2Cl_2/MeOH = 20:1), followed by PTLC purification (silica gel, CH_2Cl_2/MeOH = 20:1) to give 68.2 mg (0.145 mmol) of the title product **35** in 64% yield as a white foam.

^{1}H NMR (300 MHz, $CDCl_3$) δ 7.83–7.78 (1H, m), 7.73 (1H, dd, J = 6.96, 2.19 Hz), 7.71–7.65 (1H, m), 7.47 (1H, ddd, J = 8.43, 4.56, 2.19 Hz), 7.33–7.27 (3H, m), 4.33–4.23 (1H, m), 3.39 (2H, s), 3.26 (2H, d, J = 11.7 Hz), 2.65 (1H, br s), 2.57 (2H, q, J = 11.7 Hz), 2.37 (2H, t, J = 11.6 Hz), 1.96–1.84 (4H, m), 1.68–1.40 (12H, m). Compound **35** was converted into the corresponding dihydrochloride: ^{13}C NMR (150 MHz, CD_3OD) δ 162.7 (1C, s, J_{C-F} = 255.0 Hz), 151.8 (1C, s), 136.6 (1C, s), 134.8 (1C, d), 133.5 (1C, s), 133.1 (1C, d, J_{C-F} = 8.1 Hz), 128.1 (1C, d), 127.8 (1C, d), 124.4 (1C, s, J_{C-F} = 18.7 Hz), 124.2 (1C, s), 120.1 (1C, d, J_{C-F} = 45 Hz), 118.1 (1C, d), 116.4 (1C, d), 76.0 (1C, s), 63.4 (1C, t), 55.9 (1C, d), 48.3 (2C, t), 30.1 (2C, t), 29.1 (2C, t), 28.7 (2C, t), 27.6 (1C, t), 25.2 (2C, t). IR (KBr): 3400, 2924, 2853, 1470, 1269, 1061, 816 cm^{-1}. MS (ESI positive) m/z: $[M+H]^+$ 470.22. Anal. Calcd for $C_{27}H_{33}N_3OFCl{\cdot}2HCl{\cdot}0.5H_2O$: C, 58.75; H, 6.57; N, 7.61. Found: C, 58.74; H, 6.68; N, 7.40.

4.1.4.5. Methyl 1-aminocyclohexanecarboxylate (37). To dry MeOH (80.0 mL) was added dropwise $SOCl_2$ (21.0 mL) at −10 °C under N_2 over 15 min, and the resulting solution was stirred at −10 °C for 10 min, then 1-aminocyclohexanecarboxylic acid (11.45 g, 80.0 mmol) was added at a time. The mixture was stirred at −10 °C under N_2 for 5 min, allowed to room temperature and stirred for 6 days. The reaction solution was concentrated in vacuo, and the resulting white solid was partitioned between Et_2O (150 mL) and saturated aqueous $NaHCO_3$ (150 mL) at 0 °C. The ethereal layer was separated, and the aqueous layer was extracted with Et_2O (3× 150 mL). The ethereal layers were combined, dried over anhydrous $MgSO_4$, filtered, and concentrated in vacuo to give 11.17 g of the title product **37** in 89% yield. ^{1}H NMR (300 MHz, $CDCl_3$) δ 3.72 (3H, s), 1.98–1.87 (2H, m), 1.72–1.34 (10H, m).

4.1.4.6. Methyl 1-(4-oxopiperidin-1-yl)cyclohexanecarboxylate (38). A solution of **12** (2.87 g, 10.7 mmol) in H_2O (53.0 mL) was gradually added to a refluxing mixture of methyl 1-aminocyclohexanecarboxylate **37** (11.17 g, 71.1 mmol) and K_2CO_3 (657.9 mg, 4.76 mmol) in MeOH (122 mL) under N_2 over 50 min. The reaction mixture was stirred under reflux conditions under N_2 for 1 h. More a solution of 1-ethyl-1-methyl-4-oxopiperidinium iodide **12** (0.957 g, 3.56 mmol) in H_2O (18.0 mL) was added to the above refluxing mixture over 20 min, then additional K_2CO_3 (164 mg, 1.19 mmol) was added. The reaction mixture was stirred under reflux conditions for 1 h, allowed to room temperature, stirred for 1 day then concentrated in vacuo. The residue was mixed with H_2O (100 mL), and the mixture was extracted with CH_2Cl_2 (2× 100 mL). The combined organic extracts were dried over anhydrous $MgSO_4$, filtered, and concentrated in vacuo. The residue was purified by flash column chromatography (silica gel, hexane/AcOEt = 4:1) to give 2.155 g of the title product **38** in 63% yield from **12** as a colorless crystalline. ^{1}H NMR (270 MHz, $CDCl_3$) δ 3.68 (3H, s), 2.87 (4H, t, J = 5.94 Hz), 2.41 (4H, t, J = 6.08 Hz), 2.02–1.93 (2H, m), 1.83–1.34 (8H, m).

4.1.4.7. Methyl 1-[4-(hydroxyimino)piperidin-1-yl]cyclohexanecarboxylate (39). To a solution of **38** (2.155 g, 9.01 mmol) in dry MeOH (50.0 mL) was added a solution of $NH_2OH{\cdot}HCl$ (938.8 mg, 13.5 mmol) and AcONa (1.11 g, 13.5 mmol) in dry MeOH (50.0 mL) at room temperature under N_2. The reaction solution was stirred at room temperature under N_2 for 18 h, and concentrated in vacuo. The residue was cooled to 0 °C, basified by adding saturated aqueous $NaHCO_3$ (40 mL) at the same low temperatire, then the mixture was extracted with CH_2Cl_2 (30 mL × 4). The organic layers were combined, dried over anhydrous $MgSO_4$, filtered, and concentrated in vacuo to give 2.33 g of the title product **39** in quantitative yield (crude) as a slight yellow oil. ^{1}H NMR (300 MHz, $CDCl_3$) δ 6.79 (1H, br s), 3.67 (3H, s), 2.72–2.51 (6H, m), 2.30 (2H, t, J = 5.62 Hz), 2.02–1.88 (2H, m), 1.79–1.30 (8H, m).

4.1.4.8. Methyl 1-{4-[(2-nitrophenyl)amino]piperidin-1-yl}cyclohexanecarboxylate (41) via 40. According to the procedure for the preparation of **15**, 1.87 g of **40** was prepared as a slight brown oil (crude) from **39**. To a solution of **40** (1.87 g, crude) in dry CH_3CN (90.0 mL) was added anhydrous K_2CO_3 (1.87 g, 13.5 mmol) followed by 1-fluoro-2-nitrobenzene (1.10 mL, 10.8 mmol) at room temperature under N_2. The reaction mixture was stirred under reflux conditions under N_2 for 2 days, cooled to room temperature, and concentrated in vacuo. The residue was partitioned between CH_2Cl_2 (100 mL) and H_2O (100 mL). The organic layer was separated, and the aqueous layer was extracted with CH_2Cl_2 (3× 100 mL). The organic layers were combined, dried over anhydrous $MgSO_4$, filtered, and concentrated in vacuo. The residue was purified by flash column chromatography (silica gel, hexane/AcOEt = 7:1) to give 290.0 mg of the title product **41** as a yellow solid. ^{1}H NMR (270 MHz, $CDCl_3$) δ 8.17 (1H, dd, J = 8.56, 1.49 Hz), 8.10 (1H, br d, J = 7.26 Hz), 7.43–7.36 (1H, m), 6.85 (1H, d, J = 8.56 Hz), 6.64–6.58 (1H, m), 3.72 (3H, s), 3.59–3.46 (1H, m), 3.07–3.00 (2H, m), 2.36–2.27 (2H, m), 2.10–1.91 (4H, m), 1.75–1.26 (10H, m).

4.1.4.9. Methyl 1-{4-[2-(3-chloro-4-fluorophenyl)-1*H*-benzimidazol-1-yl]piperidin-1-yl]}cyclohexanecarboxylate (44) via 42. A mixture of **41** (200.0 mg, 0.553 mmol), Zn powder (361.7 mg, 5.53 mmol), and NH_4Cl (236.8 mg, 4.43 mmol) in MeOH (1.9 mL)–THF (3.8 mL)–H_2O (0.45 mL) was vigorously stirred at room temperature under N_2 for 20 h. The reaction mixture was filtered through a Celite pad with MeOH–THF washing, then the filtrate was concentrated in vacuo. The residue was cooled to 0 °C, then partitioned between CH_2Cl_2 (20 mL) and saturated aqueous $NaHCO_3$ (20 mL) at 0 °C. The organic layer was separated, and the aqueous layer was extracted with CH_2Cl_2 (20 mL × 3). The organic layers were combined, dried over anhydrous $MgSO_4$, filtered, and concentrated in vacuo to give 222.1 mg of methyl 1-{4-[(2-aminophenyl)amino]piperidin-1-yl}cyclohexanecarboxylate **42** (crude). To a stirred solution of 3-chloro-4-fluorobenzoic acid (122.8 mg, 0.703 mmol) and **42** (221.1 mg, crude) in anhydrous THF (6.0 mL) was added WSCI (167.0 mg, 0.871 mmol) at −20 °C under N_2. The reaction mixture was stirred at that temperature under N_2 for 5 min, warmed to 0 °C, stirred at 0 °C for 5 min, warmed to room temperature, stirred for 2 days, then cooled to 0 °C. The reaction mixture was poured into saturated aqueous $NaHCO_3$ (40 mL) at 0 °C, then the mixture was extracted with CH_2Cl_2 (4× 40 mL). The combined extracts were dried over anhydrous $MgSO_4$, filtered and concentrated in vacuo. The residue was mixed with $POCl_3$ (30.0 mL) under N_2, and the reaction mixture warmed using an oil bath (∼110 °C), stirred for 1 h, warmed to reflux (the bath temperature ∼120 °C) and stirred for 6 h. The resulting solution was cooled to room temperature, concentrated in vacuo, then the residue was coevaporated with $CHCl_3$ (10 mL). The residue was cooled to 0 °C, diluted with $CHCl_3$ (25 mL), then H_2O (20 mL) was added at 0 °C. The mixture was basified by adding 25% aqueous ammonia at the same low temperature, then the organic layer was separated, and the aqueous layer was extracted with $CHCl_3$ (2× 25 mL). The organic layers were combined, dried over anhydrous $MgSO_4$, filtered, and concentrated in vacuo. The residue was purified by PTLC (silica gel, hexane/AcOEt = 3:1) to give 78.3 mg of the title product **44** in 30% yield from **41**. ^{1}H NMR (300 MHz, $CDCl_3$) δ 7.82–7.78 (1H, m), 7.75–7.69 (2H, m), 7.46 (1H, ddd, J = 8.61, 4.38, 2.01 Hz), 7.33–7.27 (3H, m), 4.30–4.19 (1H, m), 3.69 (3H, s), 3.28 (2H, d, J = 12.1 Hz), 2.65–2.51 (2H, m), 2.13–1.30 (14 H, m).

4.1.4.10. (1-{4-[2-(3-Chloro-4-fluorophenyl)-1*H*-benzimidazol-1-yl]piperidin-1-yl}cyclohexyl)methanol (45). To a solution of **44** (78.3 mg, 0.167 mmol) in anhydrous THF (3.0 mL) was added LAH (9.5 mg, 0.25 mmol) at 0 °C under N_2. The reaction mixture was allowed to room temperature, stirred under N_2, for 2 days then

cooled to 0 °C. AcOEt (4 mL) was added to the reaction solution at 0 °C, allowed to room temperature, stirred for 1 h, cooled to 0 °C, then H_2O (10 mL) was added dropwise. The mixture was allowed to room temperature and stirred for 1 h. The organic layer was separated, and the aqueous layer was extracted with CH_2Cl_2 (4× 15 mL). The organic layers were combined, dried over anhydrous $MgSO_4$, filtered, and concentrated in vacuo. The residue was purified by flash column chromatography (silica gel, CH_2Cl_2/MeOH = 20:1) to give 50.5 mg of the title product **45** in 68% yield as a white foam. ^{1}H NMR (270 MHz, $CDCl_3$) δ 7.84–7.78 (1H, m), 7.74–7.67 (2H, m), 7.48 (1H, ddd, J = 8.49, 4.46, 1.97 Hz), 7.33–7.26 (3H, m), 4.33–4.20 (1H, m), 3.58 (2H, s), 3.24 (2H, d, J = 10.9 Hz), 2.65–2.50 (2H, m), 2.32 (2H, t, J = 11.9 Hz), 2.10 (1H, br s), 1.98–1.90 (2H, m), 1.73–1.20 (10H, m). Compound **45** was converted into the corresponding dihydrochloride: ^{13}C NMR (150 MHz, DMSO-d_6) δ 159.2 (1C, s, J_{C-F} = 252.5 Hz), 148.9 (1C, s), 134.0 (1C, s), 132.9 (1C, d), 131.7 (1C, d, J_{C-F} = 8.3 Hz), 130.8 (1C, s), 125.4 (1C, d), 125.0 (1C, d), 122.4 (1C, s), 120.4 (1C, s, J_{C-F} = 18.6 Hz), 117.8 (1C, d, J_{C-F} = 21.9 Hz), 115.9 (1C, d), 115.3 (1C, d), 68.6 (1C, s), 57.2 (1C, t), 53.4 (1C, d), 45.5 (2C, t), 27.4 (2C, t), 26.4 (2C, t), 24.1 (1C, t), 22.2 (2C, t). IR (KBr): 3400, 2943, 1468, 1267, 1178, 1059, 818, 762 cm^{-1}. MS (ESI positive) m/z: [M+H]$^+$ 442.17. Anal. Calcd for $C_{25}H_{29}N_3OFCl{\cdot}2HCl{\cdot}H_2O$: C, 56.35; H, 6.24; N, 7.88. Found: C, 56.65; H, 6.38; N, 7.80.

4.1.5. Synthesis of 46 and 47

4.1.5.1. 1-{4-[2-(4-Methylpiperazin-1-yl)-1*H*-benzimidazol-1-yl]-piperidin-1-yl}cyclooctanecarboxylic acid (46). A mixture of **22** (40.4 mg, 0.0864 mmol) and 2 N NaOH (0.21 mL, 0.42 mmol) in EtOH (4.0 mL) was stirred under reflux conditions using an oil bath (~120 °C) under N_2 for 7 h, then 2 N NaOH (0.40 mL, 0.80 mmol) and EtOH (1.0 mL) were added. The mixture was stirred under reflux conditions for 5 h, more 2 N NaOH (0.4 mL, 0.80 mmol) were added, stirred under reflux conditions for 21 h, then concentrated in vacuo. The residual slight cream solid was dissolved in H_2O (2 mL) and 2 N NaOH (4 mL) at room temperature. The resting slight amount of the starting material was washed out with CH_2Cl_2 (4× 5 mL). The aqueous solution was acidified by adding 2 N HCl (6 mL) at 0 °C, and the resulting mixture was dissolved in 2 N NaOH (3 mL) at 0 °C, then washed with CH_2Cl_2 (3× 5 mL). The aqueous layer was adjusted to pH 6 by adding 2N HCl at 0 °C, and the resulting white precipitate was collect by filtration, dried under vacuumed to afford 6.4 mg of the title product **46** as white solid. On the other hand, the volume of the above filtrate was reduced with rotary evaporator to ~15 mL. The residue, which was consisted of aqueous solution and white form-like solid, was extracted with AcOEt (4× 15 mL). The aqueous layer that included white form-like solid was extracted with CH_2Cl_2 (3× 15 mL). The combined extracts were dried over Na_2SO_4, and concentrated in vacuo to afford 11.3 mg of the product **46** as a white solid (total 45%). ^{1}H NMR ($CDCl_3$, 300 MHz) δ 7.67–7.58 (2H, m), 7.15–6.94 (2H, m), 4.16–4.02 (1H, m), 3.36–3.13 (6H, m), 2.68–1.30 (27H, m). ^{13}C NMR (150 MHz, CD_3OD) δ 175.4 (1C, s), 159.6 (1C, s), 143.2 (1C, s), 134.5 (1C, s), 123.9 (1C, d), 123.8 (1C, d), 119.8 (1C, d), 113.8 (1C, d), 79.8 (1C, s), 56.2 (2C, t), 53.9 (1C, d), 52.9 (2C, t), 49.8 (2C, t), 46.9 (1C, q), 30.2 (2C, t), 29.8 (2C, t), 29.7 (2C, t), 27.6 (1C, t), 25.9 (2C, t). MS (ESI positive) m/z: [M+H]$^+$ 454; MS (ESI negative) m/z: 452 [M−H]$^-$; HRMS-FAB m/z: exact mass calcd for $C_{26}H_{40}N_5O_2$ [M+H]$^+$, 454.3182; found, 454.3193. Anal. Calcd for $C_{26}H_{39}N_5O_2{\cdot}2.4H_2O$: C, 62.85; H, 8.89; N, 14.09. Found: C, 63.14; H, 8.60; N, 13.72.

4.1.5.2. 1-{1-[1-(Hydroxymethyl)cyclooctyl]piperidin-4-yl}-1*H*-benzimidazol-2(3*H*)-one (47). To a solution of **18** (258.0 mg, 0.669 mmol) in anhydrous THF (6.0 mL) was added LAH (38.0 mg, 1.00 mmol) at 0 °C under N_2. The reaction mixture was allowed to room temperature, stirred under N_2 for 2 h, cooled to 0 °C, and then AcOEt (4 mL) was added. The mixture was warmed to room temperature, and stirred for 1 h. The mixture was diluted with AcOEt (30 mL), then washed with H_2O (30 mL). The organic layer was separated, and the aqueous layer was extracted with AcOEt (8× 30 mL). The organic layers were combined, dried over anhydrous $MgSO_4$, filtered, and concentrated in vacuo. The residue was purified by flash column chromatography (silica gel, CH_2Cl_2/MeOH = 20:1 to 14:1) to give 157.0 mg of the title product **47** in 66% yield as a white solid. ^{1}H NMR (300 MHz, $CDCl_3$) δ 8.40 (1H, br s), 7.23–7.18 (1H, m), 7.11–7.05 (3H, m), 4.44–4.28 (1H, m), 3.36 (2H, s), 3.23 (2H, d, J = 11.0 Hz), 2.49 (2H, t, J = 11.2 Hz), 2.40–2.26 (2H, m), 1.98–1.38 (17H, m). MS (EI direct) m/z: M$^+$ 357. Compound **47** (157 mg) was converted into the corresponding hydrochloride. Mp: 248 °C. ^{13}C NMR (150 MHz, $CDCl_3$–CD_3OD = 1:1) δ 154.5 (1C, s), 128.6 (1C, s), 127.7 (1C, s), 120.7 (1C, d), 120.5 (1C, d), 109.0 (1C, d), 109.0 (1C, d), 64.1 (1C, t), 61.3 (1C, s), 51.1 (1C, d), 45.3 (2C, t), 30.0 (2C, t), 28.1 (2C, t), 28.0 (2C, t), 24.9 (1C, t), 22.1 (2C, t). IR (KBr): 3371, 3252, 2926, 1690, 1485, 1387, 1057, 756, 741 cm^{-1}. Anal. Calcd for $C_{21}H_{31}N_3O_2{\cdot}HCl{\cdot}0.4H_2O$: C, 62.88; H, 8.24; N, 10.47. Found: C, 62.97; H, 8.36; N, 10.18.

4.2. Biology

4.2.1. General

All animal experiments were conducted according to the guideline of animal care and use, and all procedures were approved by the Animal Ethics Committee in Pfizer Global Research & Development Nagoya Laboratories. The animal work was also approved by the Pfizer Institutional Animal Care and Use Committee (IACUC).

4.2.2. In vitro characterization for NOP receptor agonists

In vitro studies on hNOP receptor binding affinities and functional efficacies ([^{35}S]GTPγS assays) as well as on human classical opioid peptide receptors (MOP, KOP, and DOP receptors) binding affinities and functional efficacies were conducted.

The hNOP receptor transfected human embryonic kidney (HEK)-293 cell membranes, the hMOP receptor transfected Chinese hamster ovary (CHO)-K1 cell membranes, the hKOP receptor transfected HEK-293 cell membranes, and the hDOP receptor transfected CHO-K1 cell membranes were purchased from Receptor Biology Inc. [^{3}H]N/OFQ (150 Ci/mmol), [^{3}H]enadoline (45.0 Ci/mmol), [^{35}S]GTPγS (1060–1150 Ci/mmol) and wheatgerm agglutinin (WGA)-scintillation proximity assay (SPA) beads were obtained from Amersham Pharmacia Biotech K.K. [^{3}H]DAMGO (54.0 Ci/mmol) and [^{3}H]DPDPE (45.0 Ci/mmol) were provided from NEN Life Science Products Inc. N/OFQ was from Peptide Institute Inc. DAMGO and DPDPE were from Sigma Chemical. J-113397 was prepared by us in Pfizer Global Research & Development.

4.2.2.1. Evaluation of receptor binding affinities to hNOP receptor and human classical opioid peptide receptors (hMOP, hKOP, and hDOP receptors)[2b,21]. All competitive displacement analyses (IC_{50} and K_i) for the hNOP receptor as well as the hMOP, hKOP, and DOP receptors were performed in duplicate in a 96-well plate using a scintillation proximity assay (SPA). After the reaction, the assay plate was centrifuged at 1000 rpm for 1 min, then the radioactivity was measured by a 1450 MicroBeta (Wallac) liquid scintillation counter. IC_{50} values were calculated by non-linear regression with the software GraphPad Prism, version 4.0 (GraphPad Software, Inc., San Diego, CA). K_i values were calculated by the following equation, $K_i = IC_{50}/(1 + [L]/K_D)$, where [L] is the radiolabeled ligand concentration and K_D is the dissociation constant.

hNOP receptor binding assay. The hNOP receptor membranes (8.3 μg) were incubated at 25 °C for 45 min with 0.4 nM [^{3}H]N/OFQ, 1.0 mg of WGA-SPA beads, and six different concentrations

of compounds (10^{-11}–10^{-5} M, 10-fold) in a final volume of 0.2 mL of 50 mM HEPES buffer, pH 7.4, containing 10 mM $MgCl_2$ and 1 mM EDTA. Non-specific binding was determined by the addition of 1 μM unlabeled N/OFQ. Approximately 900 cpm of total binding were obtained, of which 3.3% was the non-specific binding.

hMOP receptor binding assay. The hMOP receptor membranes (18 μg) were incubated at 25 °C for 45 min with 1.0 nM [^{3}H]DAMGO, 1.0 mg of WGA-SPA beads, and six different concentrations of compounds (10-fold) in a final volume of 0.2 mL of 50 mM Tris–HCl buffer, pH 7.4, containing 5 mM $MgCl_2$. Non-specific binding was determined by the addition of 1 μM of unlabeled DAMGO. Approximately 240 cpm of total binding were obtained, of which 9.6% was the non-specific binding.

hKOP receptor binding assay. The hKOP receptor membranes (13 μg) were incubated at 25 °C for 45 min with 0.5 nM [^{3}H]enadoline, 1.0 mg of WGA-SPA beads, and six different concentrations of compounds (10-fold) in a final volume of 0.2 mL of 50 mM Tris–HCl buffer, pH 7.4, containing 10 mM $MgCl_2$ and 1 mM EDTA. Non-specific binding was determined by the addition of 1 μM unlabeled enadoline. Approximately 270 cpm of total binding were obtained, of which 5.6% was the non-specific binding.

hDOP receptor binding assay. The hDOP receptor membranes (18 μg) were incubated at 25 °C for 45 min with 2.0 nM [^{3}H]DPDPE, 1.0 mg of WGA-SPA beads, and six different concentrations of compounds (10-fold) in a final volume of 0.2 mL of 50 mM Tris–HCl buffer, pH 7.4, containing 5 mM $MgCl_2$. Non-specific binding was determined by the addition of 1 μM unlabeled DPDPE. Approximately 800 cpm of total binding were obtained, of which 8.8% was the non-specific binding.

4.2.2.2. Evaluation of functional activity: [^{35}S]GTPγS binding assays[2b]. Agonist stimulated binding of [^{35}S]GTPγS was investigated according to the method of SPA G-protein-coupled receptor assay provided by Amersham Pharmacia Biotech with slight modification. Each hNOP, hMOP, hKOP, hDOP receptor expressing cell membrane was suspended in assay buffer (20 mM HEPES, 100 mM NaCl, 5 mM $MgCl_2$, 1 mM EDTA, 5 μM GDP, and 1 mM DTT, pH 7.4). The membranes (the same amount to their respective receptor binding assays) were incubated at 25 °C for 30 min with 0.4 nM [^{35}S]GTPγS, 1.5 mg WGA-SPA beads, and various concentrations of compounds in duplicate in a 0.2 mL total volume. After the reaction, the assay plate was centrifuged at 1000 rpm for 2 min, and then the radioactivity was measured by a 1450 MicroBeta (Wallac) liquid scintillation counter. Non-specific binding was assessed with 10 μM of unlabeled GTPγS. Agonist stimulated binding was determined as the difference between total binding in the presence of compound and basal binding determined in the absence of compound. EC_{50} (potency) value was the concentration producing a half-maximal response of its own. E_{max} (efficacy) value was the maximal response calculated as the percentage of the maximal response produced by each control (N/OFQ, DAMGO, enadoline, and DPDPE). All the binding data were analyzed by non-linear regression with the software GraphPad Prism version 4.0 (GraphPad Software, Inc., San Diego, CA).

4.2.3. In vivo evaluation of analgesic efficacy for NOP receptor agonists in the CCI rats (von Frey hair test)

Male SD rats (7 weeks, Nippon SLC) were used (n = 5–6 for each group). Surgery of CCI (left side) was made according to the procedure of Bennett and Xie.[25] Thus, animals (220–240 g) were anesthetized with sodium pentobarbital (60 mg/kg, ip) and the left common sciatic nerve was exposed at the level of the middle of the thigh, and 4 ligatures were loosely tied around the nerve by using 4-0 chromic gut (Ethicon Inc., Brussels, Belgium). Sham operation was performed in the same manner except for sciatic-nerve ligation. On the 14th postoperative day, mechanical allodynia was evaluated by application of von Frey hairs (Semmes-Weinstein Monofilaments, North Coast Medial Inc., San Jose, CA, USA) in ascending order of force (0.0045–15.14 g) to the plantar surface of the hindpaw ipsilateral to the nerve injury (left paw). The von Frey hairs tests were applied to the paw 10 times at intervals of 1–4 s to slightly different loci within the area being tested. The first hair in the series that evoked at least one response from the ten applications was designated the paw withdrawal threshold (PWT) as a quantitative index of mechanical allodynia. The criterion response was a reflexive withdrawal that did not clearly relate to stepping. In the pre-injection of NOP receptor agonist, the response thresholds for the bending force of the injured paw were significantly lower in the CCI-operated rats than sham-operated rats ($p < 0.01$, t-test), which were confirming the presence of mechanical allodynia induced by the CCI operation of the sciatic nerve. To evaluate the antiallodynic effect of the NOP receptor agonist, the bending-force threshold against the tactile von Frey hair filament stimulus that means the sensitivity to the mechanical stimulus was measured on the ipsilateral injured hindpaw.

Inhibitory effect values against mechanical allodynia in von Frey test were calculated by the following equation:

$$\%\ \text{Inhibition} = [(50\%\ \text{marking}_{\text{drug}} - 50\%\ \text{marking}_{\text{vehicle}})/(50\%\ \text{marking}_{\text{sham}} - 50\%\ \text{marking}_{\text{vehicle}})] \times 100;\ \text{Marking} = \log 10\ \text{of}\ (10 \times\ \text{bending force in milligrams}).$$

NOP receptor agonists were dissolved in physiological saline for injection. NOP receptor agonists or vehicle (saline) was subcutaneously, intrathecally or intracerebroventricularly administered to CCI rats. Three doses of NOP receptor agonists were tested for dose-dependent assessments, that is, 1, 10, and 30 mg/kg for subcutaneous administration (compounds **1** and **27**), or 5.5, 55, and 170 nmol/site (compound **1**) or 0.55, 5.5, and 55 nmol/site (N/OFQ) for intrathecal or intracerebroventricular administration, respectively. Analgesic test (von Frey hair test) was performed at given time after drug administration. The response-change for the sensitivity to the mechanical stimulus on the contralateral uninjured (normal) hind paw (right paw) was also evaluated for the NOP receptor agonists.

4.3. Pharmacokinetic study

The apparatus of HPLC system was Agilent 1100 HPLC system, and, MS/MS system was API-300 or API-3000. The analytical column was YMC polymer 18 2.0 × 75 mm. The mobile phase consisted of 10 mM aqueous $AcONH_4$ and CH_3CN (20:80, v/v), or 0.05% aqueous TFA and CH_3CN (20:80, v/v) was run at a flow rate of 0.35 mL/min. The column temperature was at 40 °C (ambient temperature with air conditioning, 24–25 °C). The sample in column eluent was detected by MS/MS.

4.3.1. Metabolic half-life values in human liver microsomes[2c]

Test compounds (1.0 μM) were incubated in human liver microsomes (pooled human liver microsomes; protein concentration: 1.0 mg/mL) with 3.3 mM $MgCl_2$, 0.1 M $NaKHPO_4$ (pH 7.4) and NADPH-regenerating factors for various times at 37 °C on 96-deep well plates (final volume 600 μL). An aliquot of samples (50 μL) was collected at 0, 5, 15, 30, and 60 min after incubation and extracted with CH_3CN. The extracted samples were measured by HPLC/MS/MS system.

4.3.2. Pharmacokinetic profiles

Test compounds (1.0 μM) were subcutaneously administered in male SD rats at the dose of 10 mg/kg on 10% sulfobutylether-β-cyclodextrin (SBECD) solution. The concentrations of the sample

in each tissue (plasma, spinal cord, CSF or brain) was measured by HPLC–MS system at given time. Values are presented as means ± standard errors of the mean (SEM).

4.4. Evaluation of hERG potassium ion channel binding[2c]

Cell paste of HEK-293 cells expressing the hERG product was suspended in 10-fold volume of ice-cold wash buffer (50 mM Tris base, 10 mM KCl, and 1 mM $MgCl_2$, pH 7.4). The cells were homogenized using a Polytron® homogenizer (Kinematica Inc.) and centrifuged at 48,000× *g* for 20 min at 4 °C. The pellet was resuspended, homogenized, and centrifuged once more in the same manner. The resultant supernatant was discarded, and the final pellet was resuspended (10-fold volume of ice-cold wash buffer) and homogenized. The membrane homogenate was aliquoted and stored at −80 °C until use. The all manipulation was done on ice, and stock solution and equipment were kept on ice at all the time. For the saturation assay, experiments were conducted in a total volume of 200 μL in 96-well plates by Skatron method. It was determined by incubating 20 μL of [^{3}H]dofetilide and 160 μL of hERG homogenate (25–35 μg protein/well) at 22 °C for 60 min in incubation buffer. Total and non-specific bindings (in the presence of 10 μM dofetilide) were determined in duplicate in a range of [^{3}H]dofetilide concentrations (1–50 nM). The incubations were terminated by rapid vacuum filtration over 0.2% polyethyleneimine soaked glass fiber filter paper using a Skatron cell harvester followed by three washes with ice-cold filtration buffer (50 mM Tris base, 10 mM KCl, and 1 mM $MgCl_2$, pH 7.4). Receptor-bound radioactivity was quantified by liquid scintillation counting using Packard LS counter. For the competition assay, 96-well plates were used, and a final assay volume was 200 μL. Various concentrations of test compound (20 μL) were incubated in duplicate with 5 nM [^{3}H]dofetilide (36 μL), 1 mg/well SPA beads (34 μL), and 20 μg protein of hERG homogenate (110 μL) at 22 °C for 60 min in the incubation buffer. Non-specific binding was determined by 10 μM dofetilide (20 μL). After the incubation, it was left for 3 h for settling beads. Channel-bound radioactivity was quantified by scintillation counting using Wallac MicroBeta plate counter. To define the radioligand concentration, 36 μL of the radioligand was mixed with Scintillation cocktail (Packard Aquasol-2, 3.5 mL) and the radioligand was counted on a Packard liquid scintillation analyzer (TRI-CARB 2700TR). The binding data was analyzed by non-linear regression with the software GraphPad Prism version 4.0 (GraphPad Software, Inc., San Diego, CA).

4.5. Evaluation of further selectivity profiles of 1[28]

The experiments of selectivity profiles over the other receptors, transporters, ion channels, and enzymes for **1** were conducted in Cerep (Celle l'Evescault, France). The affinities and biological activities for **1** were screened at 1 μM in duplicate by use of standardized assay protocols (see Supplementary data, Table S1). The respective reference compounds were tested at several concentrations to obtain concentration–response curves to validate the experiment.

4.6. Statistical analysis

Statistical comparisons of experimental data were performed by Kruskal–Wallis one way analysis of variance on ranks followed by Tukey test or *t*-test when appropriate. For all statistical tests, differences were regarded statistically significant when the *p*-value was less than 0.05. Numerical data were analyzed using GraphPad Prism version 4.0 software (GraphPad Software, Inc., San Diego, CA).

4.7. Physicochemistry

The lipophilicity values of NOP receptor agonists were calculated as values of ACD log $D_{7.4}$, the octanol–water distribution coefficient for ionizable compounds at pH 7.4, calculated by ACD software, ACD/Laboratories 9.0 (Advanced Chemistry Development, Inc., Ontario, Canada).

Acknowledgments

We thank Yoko Matsuoka and Mineko Taguchi for elemental analysis, Dr. Shinichi Sakemi and Hideyuki Aoyama for MS measurement, and Dr. Hideo Hirai for 600 MHz NMR measurement. We are grateful to Akemi Ando for HPLC measurement of HPCOM. We express our appreciation to Sumiko Tanaka for dofetilide binding measurement and Dr. Megumi Tsuchiya for technical support of Cerep panel assays.

Supplementary data

Supplementary data associated with this article can be found, in the online version, at doi:10.1016/j.bmc.2010.07.034. These data include MOL files and InChiKeys of the most important compounds described in this article.

References and notes

1. The first original report of this study for structurally novel NOP receptor agonist as analgesic was including in the following poster and oral presentation: Hayashi, S.; Hirao, A.; Imai, A.; Sugie, Y.; Nakata, E.; Ohashi, K.; Kato, A.; Yamada, Y.; Toide, K. Novel Potent ORL1 Receptor Agonists as Anti-Anxiety Drug and Analgesic Drug. In *The 25*th *Medicinal Chemistry Symposium Abstracts*, The Pharmaceutical Society of Japan, Division of Medicinal Chemistry: Nagoya, Japan, November 29–December 1, 2006; *The 25th Medicinal Chemistry Symposium Executive Committee*, The Pharmaceutical Society of Japan, Division of Medicinal Chemistry: Tokyo, Japan, 2006, 2P-49, pp 262–263. See also Ref. 2.
2. (a) The present article is also the first publication of the original synthetic study of HPCOM and its analogues herein, and the synthetic method is different from that of MCOPPB as new-class antianxiety drug and its analogues. The details of design, synthesis, SAR, and pharmacological evaluation study of novel NOP receptor agonist MCOPPB and the different series of analogues also including in Ref. 1 have been precedently published as the series of articles, that is, Refs. 2b–d; (b) Hayashi, S.; Hirao, A.; Imai, A.; Nakamura, H.; Murata, Y.; Ohashi, K.; Nakata, E. *J. Med. Chem.* **2009**, *52*, 610; (c) Hayashi, S.; Hirao, A.; Nakamura, H.; Yamamura, K.; Mizuno, K.; Yamashita, H. *Chem. Biol. Drug Des.* **2009**, *74*, 369; (d) Hirao, A.; Imai, A.; Sugie, Y.; Yamada, Y.; Hayashi, S.; Toide, K. *J. Pharmacol. Sci.* **2008**, *106*, 361.
3. General review of neuropathic pain; also, cited literatures within: (a) Argoff, C. E. *Curr. Pain Headache Rep.* **2004**, *8*, 199; Review: (b) Ossipov, M. H.; Porreca, F. *NeuroRx* **2005**, *2*, 650; Review: (c) Maag, R.; Baron, R. *Curr. Pain Headache Rep.* **2006**, *10*, 191; Review: (d) Lickiss, J. N. *Eur. J. Pain* **2001**, *5*, Suppl. 1, 5; Review: (e) Rowbotham, M. C.; Fields, H. L. *Pain* **1989**, *39*, 129; Review: (f) Fields, H. L.; Rowbotham, M.; Baron, R. *Neurobiol. Dis.* **1998**, *5*, 209; Review: (g) Malik, R. A. *Treat. Endocrinol.* **2003**, *2*, 389; Review: (h) Milch, R. A. *Surg. Clin. North Am.* **2005**, *85*, 225; Review: (i) Kehlet, H.; Jensen, T. S.; Woolf, C. J. *Lancet* **2006**, *367*, 1618.
4. General review of analgesics with limitation: (a) McCleane, G. *CNS Drugs* **2003**, *17*, 1031; Review: (b) MacPherson, R. D. *Pharmacol. Ther.* **2000**, *88*, 163; Review: (c) MacPherson, R. D. *Drugs Today* **2002**, *38*, 135; Review: (d) Przewlocki, R.; Przewlocka, B. *Eur. J. Pharmacol.* **2001**, *429*, 79; (e) Review: Wallace, M. S. *Expert Opin. Emerg. Drugs* **2001**, *6*, 249; Review: (f) Smith, P. A.; Stebbing, M. J.; Moran, T. D.; Tarkkila, P.; Abdulla, F. A. *Drug Dev. Res.* **2002**, *54*, 140; Review: (g) Devor, M. *Curr. Pain Headache Rep.* **2004**, *8*, 187.
5. (a) Meunier, J.-C.; Mollereau, C.; Toll, L.; Suaudeau, C.; Moisand, C.; Alvinerie, P.; Butour, J.-L.; Guillemot, J.-C.; Ferrara, P.; Monsarrat, B.; Mazarguil, H.; Vassart, G.; Parmentier, M.; Costentin, J. *Nature* **1995**, *377*, 532; (b) Reinscheid, R. K.; Nothacker, H.-P.; Bourson, A.; Ardati, A.; Henningsen, R. A.; Bunzow, J. R.; Grandy, D. K.; Langen, H.; Monsma, F. J., Jr.; Civelli, O. *Science* **1995**, *270*, 792.
6. (a) Fukuda, K.; Kato, S.; Mori, K.; Nishi, M.; Takeshima, H.; Iwabe, N.; Miyata, T.; Houtani, T.; Sugimoto, T. *FEBS Lett.* **1994**, *343*, 42; (b) Mollereau, C.; Parmentier, M.; Mailleux, P.; Butour, J.-L.; Moisand, C.; Chalon, P.; Caput, D.; Vassart, G.; Meunier, J.-C. *FEBS Lett.* **1994**, *341*, 33.
7. Review: (a) Calo', G.; Guerrini, R.; Rizzi, A.; Salvadori, S.; Regoli, D. *Br. J. Pharmacol.* **2000**, *129*, 1261; Review: (b) Mogil, J. S.; Pasternak, G. W. *Pharmacol. Rev.* **2001**, *53*, 381; Review: (c) Mollereau, C.; Mouledous, L. *Peptides* **2000**, *21*, 907; (d) Nicholson, J. R.; Paterson, S. J.; Menzies, J. R. W.; Corbett, A. D.; McKnight, A. T. *Can. J. Physiol. Pharmacol.* **1998**, *76*, 304; (e) Pettersson, L. M. E.;

Sundler, F.; Danielsen, N. *Brain Res.* **2002**, *945*, 266; (f) Bridge, K. E.; Wainwright, A.; Reilly, K.; Oliver, K. R. *Neuroscience* **2003**, *118*, 513; (g) Andoh, T.; Itoh, M.; Kuraishi, Y. *NeuroReport* **1997**, *8*, 2793; (h) Berthele, A.; Platzer, S.; Dworzak, D.; Schadrack, J.; Mahal, B.; Büttner, A.; Aßmus, H. P.; Wurster, K.; Zieglgänsberger, W.; Conrad, B.; Tölle, T. R. *Neuroscience* **2003**, *121*, 629; (i) Witta, J.; Palkovits, M.; Rosenberger, J.; Cox, B. M. *Brain Res.* **2004**, *997*, 24; (j) Neal, C. R., Jr.; Akil, H.; Watson, S. J., Jr. *J. Chem. Neuroanat.* **2001**, *22*, 219.

8. (a) Yu, L.-C.; Lu, J.-T.; Huang, Y.-H.; Meuser, T.; Pietruck, C.; Gabriel, A.; Grond, S.; Pierce Palmer, P. *Brain Res.* **2002**, *945*, 88; (b) Sakurada, T.; Komatsu, T.; Moriyama, T.; Sasaki, M.; Sanai, K.; Orito, T.; Sakurada, C.; Sakurada, S. *Peptides* **2005**, *26*, 2505; (c) Nozaki-Taguchi, N.; Yamamoto, T. *Anesth. Analg.* **2005**, *100*, 1087; (d) Yamamoto, T.; Nozaki-Taguchi, N.; Kimura, S. *Brain Res.* **1997**, *754*, 329; (e) Fu, X.; Wang, Y.-Q.; Wu, G.-C. *Brain Res.* **2006**, *1078*, 212; (f) Ko, M. C. H.; Naughton, N. N.; Traynor, J. R.; Song, M. S.; Woods, J. H.; Rice, K. C.; McKnight, A. T. *Br. J. Pharmacol.* **2002**, *135*, 943; (g) Ko, M. C. H.; Wei, H.; Woods, J. H.; Kennedy, R. T. *J. Pharmacol. Exp. Ther.* **2006**, *318*, 1257.
9. (a) Yamamoto, T.; Nozaki-Taguchi, N.; Kimura, S. *Neurosci. Lett.* **1997**, *224*, 107; (b) Yamamoto, T.; Nozaki-Taguchi, N. *Anesthesiology* **1997**, *87*, 1145; (c) Hao, J.-X.; Xu, I. S.; Wiesenfeld-Hallin, Z.; Xu, X.-J. *Pain* **1998**, *76*, 385; (d) Courteix, C.; Coudoré-Civiale, M.-A.; Privat, A.-M.; Pélissier, T.; Eschalier, A.; Fialip, J. *Pain* **2004**, *110*, 236; (e) Xu, I. S.; Grass, S.; Wiesenfeld-Hallin, Z.; Xu, X.-J. *Eur. J. Pharmacol.* **1999**, *370*, 17; (f) Yamamoto, T.; Sakashita, Y. *Anesth. Analg.* **1999**, *89*, 1203.
10. (a) Sommer, C.; Schäfers, M. *Drug Discovery Today Dis. Mech.* **2004**, *1*, 441; (b) Myers, R. R.; Campana, W. M.; Shubayev, V. I. *Drug Discovery Today* **2006**, *11*, 8; (c) Sharma, B.; Bhattacharya, A.; Kumra, V. P. *J. Anaesth. Clin. Pharmacol.* **2003**, *19*, 3; (d) McLachlan, E. M.; Jänig, W.; Devor, M.; Michaelis, M. *Nature* **1993**, *363*, 543; (e) Ali, Z.; Raja, S. N.; Wesselmann, U.; Fuchs, P. N.; Meyer, R. A.; Campbell, J. N. *Pain* **2000**, *88*, 161; (f) Torebjörk, E.; Wahren, L.; Wallin, G.; Hallin, R.; Koltzenburg, M. *Pain* **1995**, *63*, 11; (g) Choi, B.; Rowbotham, M. C. *Pain* **1997**, *69*, 55; (h) Xie, Y.-K.; Xiao, W.-H. *Sci. China, Ser. B* **1990**, *33*, 663; (i) Raja, S. N.; Abatzis, V.; Frank, S. M. *Anesthesiology* **1998**, *89*, 3A, ASA Abstracts, A1083; (j) Sato, J.; Perl, E. R. *Science* **1991**, *251*, 1608; (k) Zimmer, A.; Zimmer, A. M.; Baffi, J.; Usdin, T.; Reynolds, K.; König, M.; Palkovits, M.; Mezey, É. *Proc. Natl. Acad. Sci. U.S.A.* **1998**, *95*, 2630; (l) Hylden, J. L. K.; Wilcox, G. L. *Brain Res.* **1981**, *217*, 212; (m) Seybold, V. S.; Hylden, J. L. K.; Wilcox, G. L. *Peptides* **1982**, *3*, 49; (n) Yoshimura, M.; Yonehara, N. *Neurosci. Res.* **2006**, *56*, 21; (o) Bourinet, E.; Alloui, A.; Monteil, A.; Barrère, C.; Couette, B.; Poirot, O.; Pages, A.; McRory, J.; Snutch, T. P.; Eschalier, A.; Nargeot, J. *EMBO J.* **2005**, *24*, 315; (p) Yusaf, S. P.; Goodman, J.; Gonzalez, I. M.; Bramwell, S.; Pinnock, R. D.; Dixon, A. K.; Lee, K. *Biochem. Biophys. Res. Commun.* **2001**, *289*, 402.
11. (a) Fu, X.; Zhu, Z.-H.; Wang, Y.-Q.; Wu, G.-C. *Neuroscience* **2007**, *144*, 275; (b) Bucher, B. *Naunyn-Schmiedeberg's Arch. Pharmacol.* **1998**, *358*, 682; (c) Hashiba, E.; Hirota, K.; Kudo, T.; Calo', G.; Guerrini, R.; Matsuki, A. *Naunyn-Schmiedeberg's Arch. Pharmacol.* **2003**, *367*, 342; (d) Giuliani, S.; Maggi, C. A. *Br. J. Pharmacol.* **1996**, *118*, 1567; (e) Stanfa, L. C.; Chapman, V.; Kerr, N.; Dickenson, A. H. *Br. J. Pharmacol.* **1996**, *118*, 1875; (f) Luo, C.; Kumamoto, E.; Furue, H.; Chen, J.; Yoshimura, M. *Neuroscience* **2002**, *109*, 349; (g) Altier, C.; Khosravani, H.; Evans, R. M.; Hameed, S.; Peloquin, J. B.; Vartian, B. A.; Chen, L.; Beedle, A. M.; Ferguson, S. S. G.; Mezghrani, A.; Dubel, S. J.; Bourinet, E.; McRory, J. E.; Zamponi, G. W. *Nat. Neurosci.* **2006**, *9*, 31.
12. (a) Meis, S. *Neuroscientist* **2003**, *9*, 158; (b) Häbler, H.-J.; Timmermann, L.; Stegmann, J.-U.; Jänig, W. *Br. J. Pharmacol.* **1999**, *127*, 1719; (c) Bartsch, T.; Akerman, S.; Goadsby, P. J. *Neuropharmacology* **2002**, *43*, 991; (d) Peiser, C.; Undem, B. J.; Fischer, A. *Peptides* **2000**, *21*, 995; (e) Lee, M.-G.; Undem, B. J.; Brown, C.; Carr, M. J. *Am. J. Respir. Crit. Care Med.* **2005**, *173*, 271; (f) Polidori, C.; Massi, M.; Guerrini, R.; Grandi, D.; Lupo, D.; Morini, G. *Endocrinology* **2005**, *146*, 3861.
13. Cremlyn, R. J. W.; Chisholm, M. *J. Chem. Soc. C* **1967**, *22*, 2269.
14. Tschaen, D. M.; Abramson, L.; Cai, D.; Desmond, R.; Dolling, U.-H.; Frey, L.; Karady, S.; Shi, Y.-J.; Verhoeven, T. R. *J. Org. Chem.* **1995**, *60*, 4324.
15. Radesca, L.; Bowen, W. D.; Di Paolo, L.; de Costa, B. R. *J. Med. Chem.* **1991**, *34*, 3058.
16. TenBrink, R. E.; Im, W. B.; Sethy, V. H.; Tang, A. H.; Carter, D. B. *J. Med. Chem.* **1994**, *37*, 758.
17. Morita, S.; Kitano, K.; Matsubara, J.; Ohtani, T.; Kawano, Y.; Otsubo, K.; Uchida, M. *Tetrahedron* **1998**, *54*, 4811.
18. (a) Ohnmacht, C. J., Jr.; Draper, C. W.; Dedinas, R. F.; Loftus, P.; Wong, J. J. *J. Heterocycl. Chem.* **1983**, *20*, 321; (b) See also a late example of large scale synthesis for the compound: Colon-Cruz, R; Didiuk, M. T.; Duffy, E. M.; Garigipati, R. S.; Lau, W. F.; McDonald, W. S. International Patent WO 02070523 September 12, 2002.
19. Gravatt, G. L.; Baguley, B. C.; Wilson, W. R.; Denny, W. A. *J. Med. Chem.* **1994**, *37*, 4338.
20. (a) Shoblock, J. R. *CNS Drug Rev.* **2007**, *13*, 107; (b) Varty, G. B.; Lu, S. X.; Morgan, C. A.; Cohen-Williams, M. E.; Hodgson, R. A.; Smith-Torhan, A.; Zhang, H.; Fawzi, A. B.; Graziano, M. P.; Ho, G. D.; Matasi, J.; Tulshian, D.; Coffin, V. L.; Carey, G. J. *J. Pharmacol. Exp. Ther.* **2008**, *326*, 672.
21. Cheng, Y.-C.; Prusoff, W. H. *Biochem. Pharmacol.* **1973**, *22*, 3099.
22. Ozaki, S.; Kawamoto, H.; Itoh, Y.; Miyaji, M.; Azuma, T.; Ichikawa, D.; Nambu, H.; Iguchi, T.; Iwasawa, Y.; Ohta, H. *Eur. J. Pharmacol.* **2000**, *402*, 45.
23. (a) Lin, J. H.; Lu, A. Y. H. *Pharmacol. Rev.* **1997**, *49*, 403; (b) van de Waterbeemd, H.; Smith, D. A.; Jones, B. C. *J. Comput. Aided Mol. Des.* **2001**, *15*, 273; (c) Lee, P. H.; Cucurull-Sanchez, L.; Lu, J.; Du, Y. J. *J. Comput. Aided Mol. Des.* **2007**, *21*, 665.
24. Hirao, A.; Imai, A.; Sugie, Y.; Tamura, T.; Shimokawa, H.; Toide, K. *Eur. J. Pharmacol.* **2008**, *579*, 189.
25. Bennett, G. J.; Xie, Y.-K. *Pain* **1988**, *33*, 87.
26. (a) Kato, A.; Nakazato, E. *Jpn. J. Pharmacol.* **2001**, *85*, Suppl. 1, 224P, P-660; See also independent study reports as follows: (b) Briscini, L.; Corradini, L.; Ongini, E.; Bertorelli, R. *Eur. J. Pharmacol.* **2002**, *447*, 59; (c) Corradini, L.; Briscini, L.; Ongini, E.; Bertorelli, R. *Brain Res.* **2001**, *905*, 127.
27. Al-Khatib, S. M.; LaPointe, N. M. A.; Kramer, J. M.; Califf, R. M. *JAMA J. Am. Med. Assoc.* **2003**, *289*, 2120.
28. See also the methods and references that can be found on the Cerep website (www.cerep.fr).
29. Narita, M.; Mizoguchi, H.; Oji, D. E.; Narita, M.; Dun, N. J.; Hwang, B. H.; Nagase, H.; Tseng, L. F. *Br. J. Pharmacol.* **1999**, *128*, 1300.
30. Mika, J.; Schäfer, M. K. H.; Obara, I.; Weihe, E.; Przewlocka, B. *Pharmacol. Biochem. Behav.* **2004**, *78*, 171.
31. (a) Chen, Y.; Sommer, C. *J. Peripher. Nerv. Syst.* **2006**, *11*, 232; (b) Jia, Y.-p.; Linden, D. R.; Serie, J. R.; Seybold, V. S. *Neurosci. Lett.* **1998**, *250*, 21; (c) Ma, F.; Xie, H.; Dong, Z.-Q.; Wang, Y.-Q.; Wu, G.-C. *Brain Res.* **2005**, *1043*, 214.
32. (a) Inoue, H.; Matsunaga, S.; Rashid, M. H.; Yoshida, A.; Mizuno, K.; Sakurada, T.; Takeshima, H.; Ueda, H. *J. Pharmacol. Exp. Ther.* **2001**, *299*, 213; (b) Watanabe, H.; Mizoguchi, H.; Orito, T.; Katsuyama, S.; Yonezawa, A.; Watanabe, C.; Sakurada, T.; Sakurada, S. *Peptides* **2007**, *28*, 670.
33. (a) Obara, I.; Przewlocki, R.; Przewlocka, B. *Pain* **2005**, *116*, 17; (b) Chiou, L.-C.; Chuang, K.-C.; Wichmann, J.; Adam, G. *J. Pharmacol. Exp. Ther.* **2004**, *311*, 645; (c) Rizzi, D.; Bigoni, R.; Rizzi, A.; Jenck, F.; Wichmann, J.; Guerrini, R.; Regoli, D.; Calo', G. *Naunyn-Schmiedeberg's Arch. Pharmacol.* **2001**, *363*, 551.
34. (a) Mathis, J. P.; Ryan-Moro, J.; Chang, A.; Hom, J. S. H.; Scheinberg, D. A.; Pasternak, G. W. *Biochem. Biophys. Res. Commun.* **1997**, *230*, 462; (b) Xie, G.-x.; Ito, E.; Maruyama, K.; Pietruck, C.; Sharma, M.; Yu, L.-C.; Palmer, P. P. *Brain Res. Mol. Brain Res.* **2000**, *77*, 1; (c) Terenius, L.; Sandin, J.; Sakurada, T. *Peptides* **2000**, *21*, 919.
35. (a) Lapalu, S.; Moisand, C.; Butour, J.-L.; Mollereau, C.; Meunier, J.-C. *FEBS Lett.* **1998**, *427*, 296; (b) Pan, Y.-X.; Bolan, E.; Pasternak, G. W. *Biochem. Biophys. Res. Commun.* **2002**, *297*, 659; (c) Bhushan, R. G.; Sharma, S. K.; Xie, Z.; Daniels, D. J.; Portoghese, P. S. *J. Med. Chem.* **2004**, *47*, 2969; (d) Waldhoer, M.; Fong, J.; Jones, R. M.; Lunzer, M. M.; Sharma, S. K.; Kostenis, E.; Portoghese, P. S.; Whistler, J. L. *Proc. Natl. Acad. Sci. U.S.A.* **2005**, *102*, 9050.